ELSEVIER

Journal of Marine Systems 7 (1996) 293-320

JOURNAL OF MARINE SYSTEMS

Coastal/deep ocean interactions in the Black Sea and their ecological/environmental impacts

H.İ. Sur [a,*], E. Özsoy [a], Y.P. Ilyin [b], Ü. Ünlüata [b]

[a] Institute of Marine Sciences, Middle East Technical University, P.K. 28, Erdemli, İçel 33731, Turkey
[b] Ukrainian Academy of Sciences, Marine Hydrophysical Institute, 2, Kapitanskaya Str., Sevastopol 33500 Crimea, Ukraine

Received 11 July 1994; accepted 17 April 1995

Abstract

Satellite (CZCS, AVHRR) and in-situ (CTD, ADCP) data are utilized to characterize the impact of meso-scale motions and boundary currents on transport and productivity along the wide Western Black Sea Shelf.

Various forms of isolated transient features including filaments, coherent dipole and monopole eddies and jets transport materials and momentum across the continental shelf. Unstable meandering motions generated at topographic irregularities propagate along the continental slope. As a result of the meandering motions, the material transported spreads into an area several times wider than the continental shelf/slope region.

The spring-time surface productivity in the southern Black Sea is modulated by transient dynamics. Species differentiation and competition are evident along the boundary current system. Early summer plankton blooms coincide with peak flood discharges from major rivers, and influence the spread of eutrophication in the basin.

Upwelling patches are evident along the west Anatolian coastline, in response to transient surface divergence. The upwelling locally has an adverse effect on fish eggs and larvae.

In winter, cold water is formed on the western continental shelf. As the band of cold water follows the coast and interacts with coastal geometry, it leads to winter plankton blooms, particularly along the southern coast.

Coherent meso-scale/synoptic eddies and turbulent features are shown to evolve rapidly in the system, indicating rapid conversions between different forms of energy in the upper layers of the ocean.

1. Introduction

In the energetic environment of the Black Sea, in-situ measurements with sufficient space and time resolution are required to describe the rapidly changing meso-scale and sub-meso-scale fields. A detailed, time dependent description of the surface features is furnished by satellite remote sensing, and a sufficient understanding of the productivity and transport mechanisms is obtained by a synthesis of remote sensing and in-situ data.

The high spatial frequency of ocean surface sampling with imaging sensors has motivated investigations of complex oceanic processes. Diurnal solar heating can often mask the ocean surface temperature in infra-red data, destroying any correlations with underlying dynamical features

* Corresponding Author

SSDI 0924-7963(95)00030-5

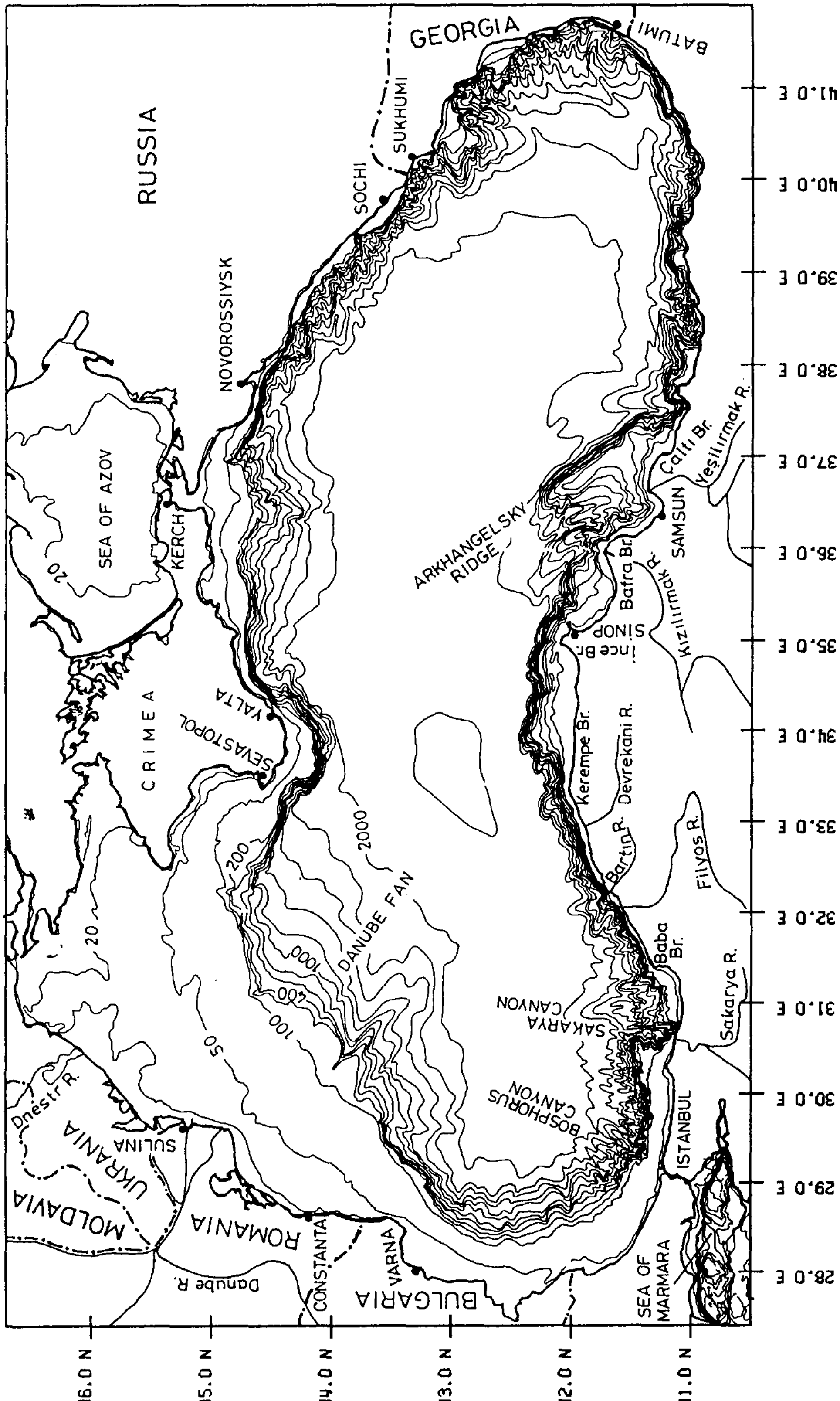

Fig. 1. Bathymetry and location map of the Black Sea.

(e.g. Deschamps and Frouin, 1984), and the surface mixed layer temperatures can be uniform in relatively large areas of the ocean. As a result, many ocean flow features can be visualized by color data even when they do not appear on infra-red imagery (e.g. Ahlnäs et al., 1987). The ocean surface circulation is better resolved by the CZCS (Coastal Zone Color Scanner) data, which represents a depth comparable to the attenuation distance of visible light, although the phytoplankton pigments measured are not conservative tracers (Yentsch, 1984). In this way, the CZCS data picks up regions of increased fertility, which are typically the boundaries of major ocean currents or eddies.

We use satellite and in-situ data together to identify dynamical processes associated with the meandering boundary currents and to discuss their impacts on the biochemical cycles in the Black Sea. Earlier discussions of the Black Sea circulation and transport based on satellite data have been given by Oğuz et al. (1992) and Sur et al. (1994).

Unstable meanders, filaments, coherent dipole eddies or paired eddies with opposite signed vorticity, similar to those found in the Black Sea, have been studied along density-driven boundary currents in many parts of the world ocean: the reader is referred to Fedorov and Ginsburg (1989) for a review of dipole vortices, and to Qiu et al. (1988), Chao (1990), Millot (1991) and Beckers and Nihoul (1992) for unstable boundary currents and examples of associated upwelling.

The meandering and filamented structures of boundary currents are of primary importance in determining the exchange between the shelf regions and the deep ocean, with many bio–geochemical implications. In a basin of relatively small size such as the Black Sea, cross-shelf exchanges are of central importance because (i) occasionally the horizontal scales in the bursts of exchanges are almost of the same scale as the basin itself, (ii) a significant amount of the fresh water, nutrients and other materials are input from major rivers (e.g. the Danube), and advected along the coast by the boundary current and then injected into the basin interior via turbulent exchanges.

2. Data and methods

Nimbus-7 CZCS and NOAA-10, 11 AVHRR images and the available in-situ data are used together to deduce the flow characteristics of the Black Sea boundary current.

All of the Nimbus-7 and NOAA-10 images received before 1994 were processed by the SEAPAK interactive processing system at the Institute of Marine Sciences–Middle East Technical University (IMS-METU). Images directly received by the HRPT station based at the IMS-METU, beginning in 1994 were processed by the MapiX *Ocean* software package. More than 100 relatively cloud free or low cloud images from the Nimbus-7 CZCS and NOAA AVHRR were examined.

For the NOAA-11 (Channel-4) images in 1992 and 1993, software developed in the Marine Hydrophysical Institute was used for pre-processing, geographical positioning and geometrical projections. Their spatial resolution is 1′ along meridian and 1.5′ along parallel, and radiation temperature resolution is about 0.1°C. Final contrast enhancements, coast and bathymetry superposition were performed at the IMS-METU.

In-situ CTD data from international cruises in the framework of HydroBlack (September, 1991) and CoMSBlack (July, 1992 and April, 1993) (Oğuz et al., 1993, 1994, 1995; Sur et al., 1994) were used to complement the satellite observations. During the CoMSBlack-93 cruise, ADCP current measurements were performed on board the R/V *Bilim* both at hydrographic stations and along the ship track.

3. General characteristics the Black Sea

3.1. Bottom topography

The bottom topography of the Black Sea (Fig. 1) displays an abyssal plain separated from the margins by steep continental slopes, except near the Danube and Kerch Fans. The wide northwestern continental shelf occupies the region between the Crimean peninsula and the west coast, and extends along the western and southwestern coasts of the Black Sea, with a shelf break depth of 100 m. The shelf becomes abruptly terminated at Sakarya Canyon where the depth suddenly increases from 100 m to about 1500 m along the Anatolian coast east of the Bosphorus. The canyon is delimited by Baba Burnu (Cape Baba) on its east, where the coast makes a sharp turn. Smaller continental shelf areas are found along the coast between the two Capes of Kerempe Burnu and Bafra Burnu, along the coast of Kerch, and at narrow stretches separated by canyons along the eastern coast.

A steep continental slope topography is located adjacent to the coast, along the coast from Sakarya Canyon to C. Kerempe. The cross-shore depth profile changes from a flat, step shaped continental shelf topography west of the Sakarya Canyon to a steep linearly deepening profile following the coastline between Sakarya Canyon and C. Kerempe, and back to the step-like shelf profile west of C. Kerempe. These transitions in bottom topography can induce significant control on the dynamics of the boundary currents.

The bottom topography becomes complicated near the Arhangelsky ridge, then the continental slope topography undulates between shallow and deep regions along the remaining eastern Black Sea coast. The continental slope region is intersected by numerous canyons throughout the Black Sea.

3.2. Circulation

The general circulation of the Black Sea is described as a basin scale cyclonic boundary current (the so-called Rim Current, Oğuz et al., 1993), which is divided into two large cyclonic gyres in the east and west, with smaller scale circulations between them, and in the easternmost corner of the basin. The strong boundary current limits the water and material transfer across the flow, while jet instabilities, mesoscale eddies, filaments, mushroom-like structures and similar phenomena play important roles in the cross-shelf (cross-frontal) exchanges.

Recent measurements (Oğuz et al., 1992, 1993, 1994) confirmed a well-defined cyclonic boundary current following the narrow continental slope and indicated a series of anticyclonic eddies

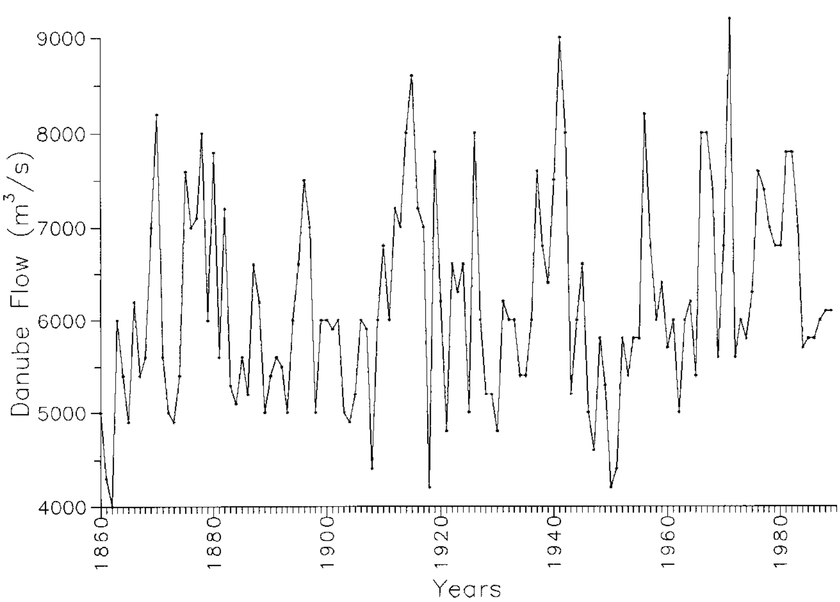

Fig. 2. Long-term measurements of annual average Danube discharge (after Bondar, 1989).

trapped between the current and the irregular coastline. Stanev et al. (1990), Latun (1990) and Eremeev et al. (1992) indicate that circulation is better defined and more intense in winter than in summer; in summer, more eddy activity is generated in a wide range of scales, and persisting either for short periods or on a seasonal basis. Some of the eddies are associated with the meandering boundary current, others are produced by atmospheric forcing and buoyancy fluxes.

It is not clear what physical factors drive the Black Sea circulation. Classically, the cyclonic pattern of winds has been recognized as the main reason for the cyclonic surface circulation (e.g. Neumann, 1942; Moskalenko, 1976). On the other hand, numerical studies by Marchuk et al. (1975) and Stanev (1990) indicate a seasonal thermohaline circulation driven by nonuniform surface fluxes, complementary to the wind driven circulation.

The northwestern shelf and the Bosphorus vicinity are the two major areas where lateral sources and convection modify the Black Sea circulation. The competing effects of freshwater inflow and winter cooling respectively create and destroy vorticity in the first area (Stanev, 1990), while intermediate depth intrusions driven by shelf mixing of the dense Mediterranean inflow creates similar disturbances in the second area (Stanev, 1990; Özsoy et al., 1993).

3.3. River inputs

Major rivers (the Danube, Dnepr and Dnestr) discharge into the northwest shelf of the Black Sea. The Danube River alone is the greatest contributor of river runoff into the Black Sea, accounting for about one half of the total riverine influx. The annual mean discharge of the Danube, monitored for more than a century (Fig. 2) indicates large natural variations within a range of 4000–9000 m^3/s. In addition to this interannual variability, seasonal changes of about $\pm 30\%$ of the annual mean occur in the discharge (Sur et al., 1994).

Salinity observation near the Anatolian coast suggest that the freshwater from the northwest shelf reaches the southwest coast. Daily measurements in the Bosphorus indicate the more prominent salinity minima during summer, from June till September (Acara, 1958; Artüz and Uğuz, 1976). The mean travel time between the Danube and the Bosphorus is calculated to be on the order of 1–2 months if a mean current speed of 10–20 cm/s is assumed for a length scale of about 500 km. Sur et al. (1994) computed the mean salinity of the surface waters within the upper 10 m in the southwestern Black Sea (between 28 and 32°E, and 41 and 42°N) from the CTD data. The weight of the data indicates a mean salinity of about 18 in the southwest sector of the Black Sea. The salinity decreases to 16–17, when the Danubian influence is felt in the area. The minimum salinity periods occur from March to August, with a large year to year variability in timing and magnitude, resulting from mixing and dispersion effects.

3.4. Productivity and eutrophication

The Black Sea is known to be a region of moderate to high productivity since it is fed by a rich supply of nutrients compared with other parts of the world ocean (Koblentz-Mishke et al., 1970). Sorokin (1983) indicated that the peaks in primary productivity of the Black Sea were known (before the last decade) to occur twice a year, with a major bloom of mainly diatoms in early spring, followed by a secondary bloom of mainly coccolithophorids in autumn. Occasional blooms of coccoliths and dinoflagellates occurred mainly in coastal areas. Recently, additional summer blooms with predominance of dinoflagellates and coccoliths (*Emiliana huxleyi*) have increasingly been observed in the region (Bologa, 1986; Benli, 1987; Hay and Honjo, 1989; Hay et al., 1990, 1991). Sorokin (1983) also reported the spring and summer development of red tides in the western shelf. Massive red tides have been created along the Rumanian and Bulgarian coasts by dinoflagellates (Tumantseva, 1985 and Sukhanova et al., 1988, and references cited therein). There are limited observations in winter, some of which indicate massive blooms of certain plankton species along the western Anatolian coast (Sur et al., 1994).

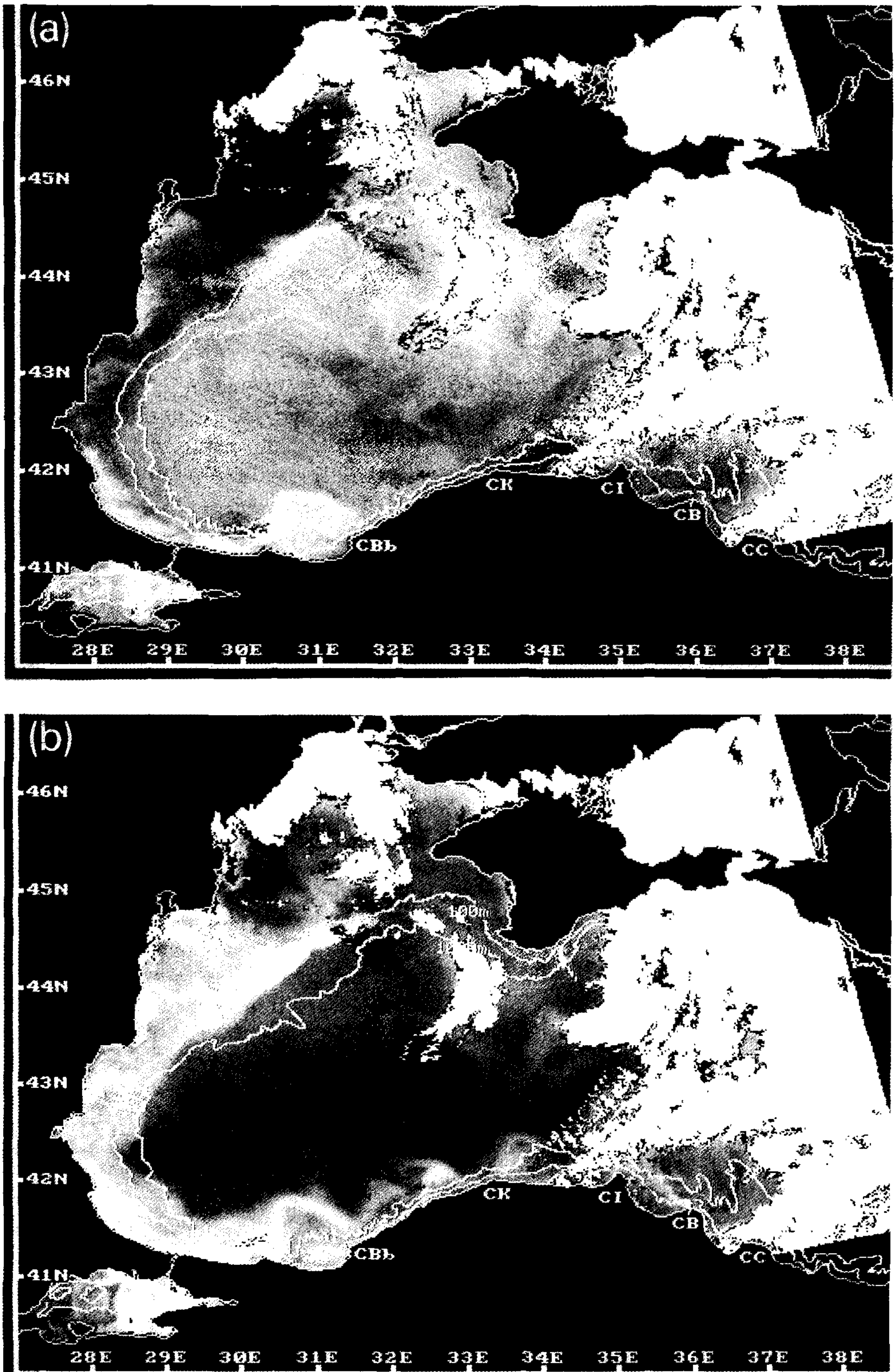
(a)
46N
45N
44N
43N
42N
41N
CK
CI
CB
CBb
CC
28E
29E
30E
31E
32E
33E
34E
35E
36E
37E
38E
(b)
100m
46N
45N
44N
43N
42N
41N
CK
CI
CB
CBb
CC
28E
29E
30E
31E
32E
33E
34E
35E
36E
37E
38E

The maximum spring–autumn primary productivity (60% of the Black Sea production) is found in the northwest shelf where 87% of the total fresh water input reaches the Black Sea from major rivers contributing large amounts of nutrients and detritus onto the shallow shelf region, reducing the surface salinity and transparency ($< 60\%$ of the total incident radiation reaching below 1 m depth). Open sea primary productivity at the centers of the western and eastern gyres of the Black Sea are typically low. Next to the high productivity areas in the northwest shelf and the northeast regions, the highest primary productivity is reported to occur along the Anatolian (southwestern) and the Romanian (western) coasts, and extends into the central region separating the eastern and western gyres (Bologa, 1986). Limited observations suggest that the western Anatolian coast is also a region of relatively high productivity (Sur et al., 1994).

The eutrophication has started in the northwestern shelf area influenced by the Danube and Dnestr river mouths (Tolmazin, 1985), and progressed south, along the western shelf (Musayeva, 1985; Bologa, 1986). The Danube introduces 60,000 t/yr of total phosphorus and about 340,000 t/yr of total inorganic nitrogen to the Black Sea at present, representing large increases in the last two decades (Mee, 1992). The major Turkish rivers are estimated to contribute only 1700 t/yr of orthophosphate and 25,000 t/yr of total inorganic nitrogen (Özsoy et al., 1992), and the labile nutrient export versus import through the Bosphorus roughly balance each other (Polat and Tuğrul, 1995).

The eutrophication has increased sharply in the last decade. Historical Secchi disc readings in the central parts of the Black Sea has decreased from 20 m in the 1920's to about 15 m until the mid-1980's and then to 5–6 m in the early 1990's (Eremeev et al., 1992). Serious decreases have occurred in the total stocks and species of fish, many organisms have disappeared from the region, and part of the food web has been invaded by opportunistic species imported from outside the region (Zaitsev, 1991). Tuğrul et al. (1992) and Saydam et al. (1992) showed that the nutrient distribution has changed drastically in the entire basin indicating that ammonia and silicate have been depleted in the near surface waters by increased utilization in the last few decades.

Murray et al. (1994) suggest that no new nitrogen seems to reach the euphotic zone from the deep water although the recycling mechanisms of nutrients within the basin are not clearly identified. Therefore, the atmospheric and riverine supply could be the main sources of new production in the Black Sea.

4. Analysis of satellite and in-situ data

4.1. Meandering flow and summer plankton blooms along the western shelf

Remarkable dynamical processes of shelf – open ocean interaction, with important impacts on productivity are investigated in Fig. 3–7. In these figures, a summer plankton bloom was in progress, originating from the northern shelf and extending into part of the interior and the entire western shelf region. Different bands of the CZCS image are shown for June 12 in Fig. 3a–d. The Channel 1 (443 nm) data indicates a dark band covering the entire western shelf, indicating absorbance of sunlight by chlorophyll-a, i.e. a massive bloom limited to the shelf. Light absorption is maximum in the northwestern shelf region near the Danube mouth, with decreasing values observed along the entire western shelf (Fig. 3a). A region of reflectance (lighter tone) is also identi-

Fig. 3. Coastal Zone Color Scanner (CZCS) satellite images on June 12, 1980. The images represent the atmospherically corrected (a) channel 1 (443 nm), (b) channel 3 (550 nm), (c) the calculated pigment concentration and (d) thermal infra-red channel. Abbreviations used; *CBb*: Cape Baba, *CK*: Cape Kerempe, *CI*: Cape İnce, *CB*: Cape Bafra, *CC*: Cape Çaltı. (In this and the following thermal images, the darker tones represent warmer and the lighter tones represent colder values.)

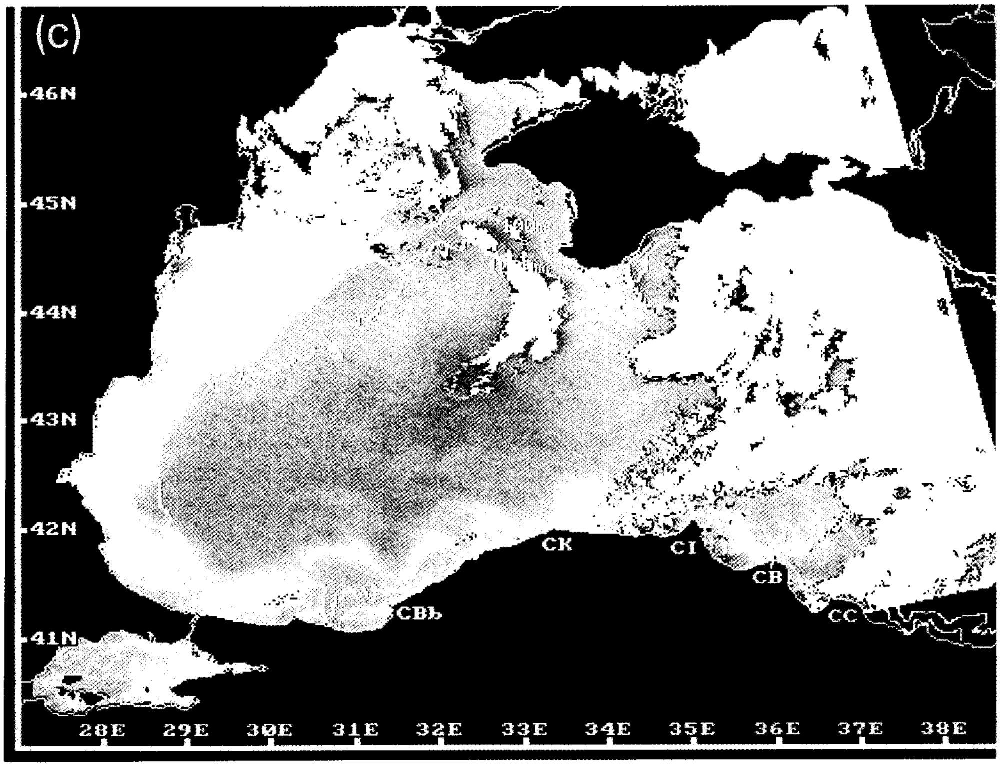
(c)
46N
45N
44N
43N
42N
41N
CK
CI
CB
CBb
CC
28E
29E
30E
31E
32E
33E
34E
35E
36E
37E
38E

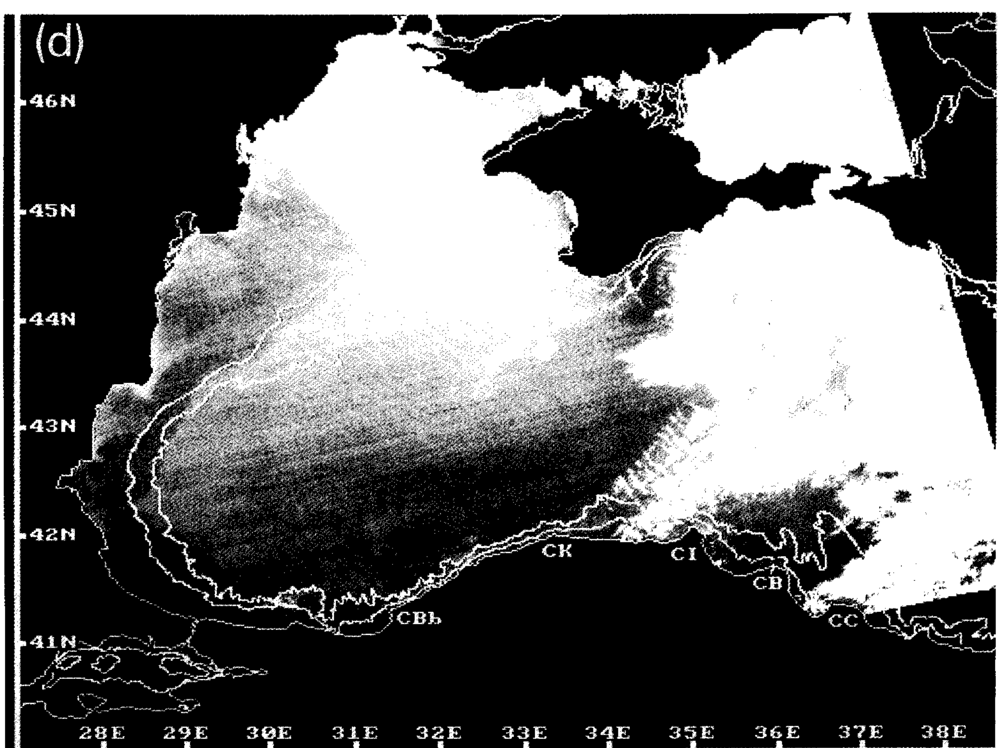
(d)
46N
45N
44N
43N
42N
41N
CK
CI
CB
CBb
CC
28E
29E
30E
31E
32E
33E
34E
35E
36E
37E
38E

fied at the front separating the shelf water from the interior. Channel 3 (550 nm) of the CZCS image (Fig. 3b) indicates particulate material in the western shelf. By using the "branching" algorithm of Gordon et al. (1983), calculated pigment distribution in Fig. 3c together with the information given by Fig. 3a, b indicates that the particulates are mainly phytoplankton. The infrared image in Fig. 3d displays a relatively warmer band of shelf water compared to the interior, outlining the convergence region where warm surface water accumulates at the coast in agreement with the cyclonic basin circulation (although the accuracy of the thermal data from this sensor is questionable, Robinson, 1991).

Multiple species of plankton can be identified in these visible bands (Figure 3a–c). The high reflectance regions in all visible bands is most likely to be populated with *E. huxleyi* (Holligan et al., 1983). As a result, we distinguish two populations of plankton, one occupying the western shelf region and the other populating the outer edge of the first group in the offshore frontal region.

Three days later (Fig. 4), we observe that the frontal region occupied by *E. huxleyi* has become unstable, ejecting a large filament (of size 150 km) from the northwest shelf region into the interior. In Figs. 5 and 6, seven and ten days later respectively, the filament preserves its identity, but a dipole eddy (with a better defined cyclonic member) develops near its cap, and the entire filament on these last two images become a region of high spectral reflectance. We also note that the region of absorption (Channel 1) initially covering the entire northwest shelf and extending south to cover the western shelf partially has become smaller and more confined to the Danube mouth in the later images.

The above observations seem to suggest competition between the shelf species and the coccolithophore bloom on its periphery. Initially the high reflectance species at the shelf edge forms a contrast with the other species distributed on the shelf region. In the following images, the shelf species are observed to become more confined, and the high reflectance species dominate the entire region excluding the vicinity of river mouths. This observed segregation behavior is typically encountered amongst similar but competing species (Okubo, 1980).

The uniform distribution of tracers observed along the western shelf, in Fig. 3b, c, verifies a cyclonic boundary current, which is replaced by undulating features east of Sakarya Canyon. During early development (Fig. 3) the wave pattern is regular, though filaments with offshore extensions are visible near C. Kerempe. 10 days later (Fig. 5), the meander has developed into a train of cyclonic and anticyclonic regions with a complex pattern of filaments extending offshore. In fact, the overall appearance of the motion in Fig. 5 is suggestive of a turbulent jet flow, with numerous meanders and filaments constituting its core. This jet follows the western Anatolian coast from Sakarya Canyon to C. Kerempe, where it begins to become separated from the coast. Note also that in the region from C. Kerempe to C. Bafra a wide continental shelf has replaced the steep bottom topography adjacent to the coast upstream. Only 3 days later, the jet flow has become wider and totally separated from the coast east of C. Kerempe (Fig. 6), and terminated with a dipole-like cap extending to the mid-basin region east of C. İnce. We observe numerous cyclonic and anticyclonic eddies within this fully developed turbulent jet.

The meandering currents along the Anatolian coast with efficient dispersion result in a massive plankton bloom, which serves to visualize the motions transporting them. The eastward propagation speed of the meandering motion is calculated to be 10–15 cm/s along the Anatolian coast (Fig. 7). Rapidity of the development is clear in

Fig. 3. (continued).

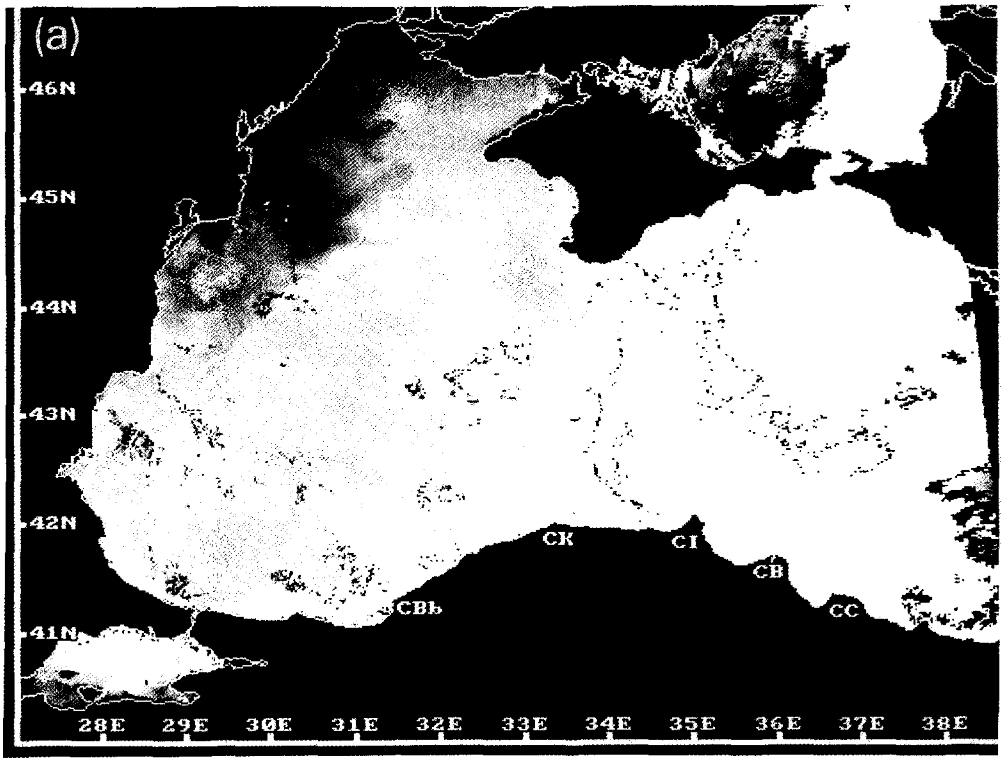

(a)
46N
45N
44N
43N
42N
41N
CK
CI
CB
CC
CBb
28E
29E
30E
31E
32E
33E
34E
35E
36E
37E
38E

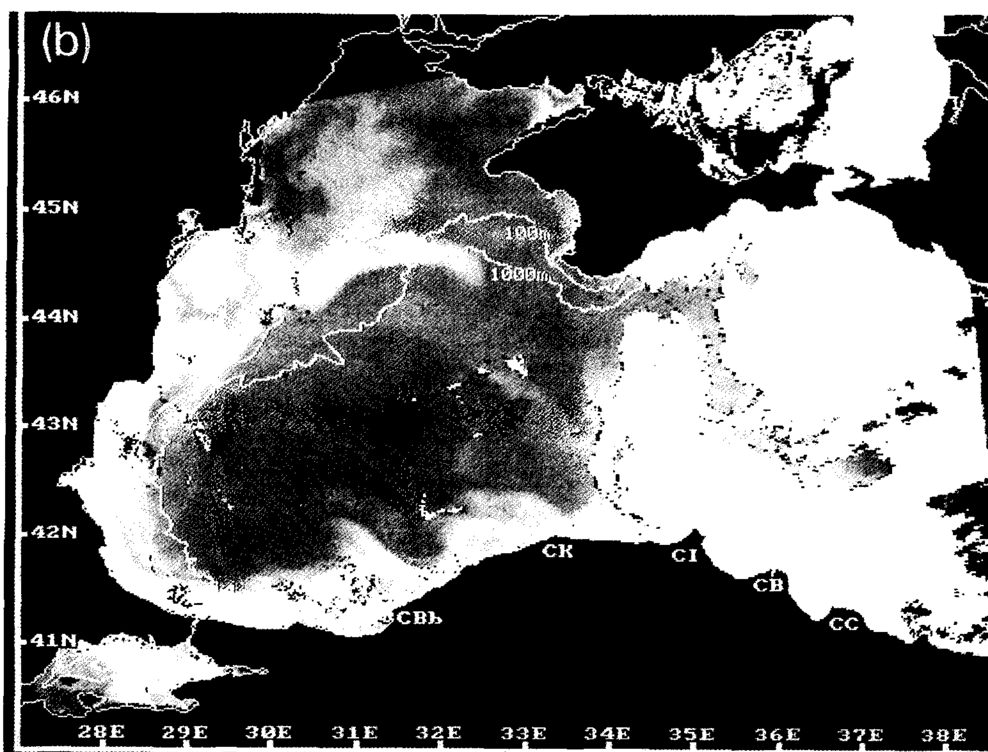

(b)
46N
45N
44N
43N
42N
41N
100m
1000m
CK
CI
CB
CC
CBb
28E
29E
30E
31E
32E
33E
34E
35E
36E
37E
38E

Figs. 3–7, an entire current system is modified in character, and unstable eddies and filaments developed within a time scale of a few days.

In Figs. 3–7, the eastern terminus of the shelf at Sakarya Canyon acts as the generation region for the eastward propagating wave motion, which indicates close correlation with the continental slope topography. The flow along the western shelf is most probably in geostrophical balance, following the bathymetric contours of the shelf/slope region. Once triggered by the sudden depth change at Sakarya Canyon, the resultant motions are unstable along the remaining part of the coast. With increasing time, the jet flow becomes wider and more turbulent with distance from the step.

Although we observe that the meandering motion of the west Anatolian boundary current is triggered by a discontinuity in shelf topography, baroclinic instability appears to contribute to its subsequent growth explaining unstable motions in buoyant coastal flows. Stern (1980) examined the instability of fronts leading to large meanders, bores or breaking waves leading to exchanges across the front, as indicated by the large excursions in Figs. 3–7. A significant amount of entrainment is noticeable from the growing sizes of the eddies.

Mysak and Schott (1977), Griffiths and Linden (1981), Ikeda et al. (1984, 1989), Qiu et al. (1988), Chao (1990), Beckers and Nihoul (1992) showed instabilities of boundary flows with horizontal density gradients. In many cases the unstable waves grow into large amplitude meanders or paired coherent vortices enhancing the cross-shelf exchanges. Chao (1990) argued that fronts in which isobaths and isopycnals slanted in opposite senses (such as in the Black Sea) are less responsive to baroclinic instability than the opposite case of upwelling fronts. However, it was demonstrated that enhanced meander and eddy growth could occur due to relaxation processes, e.g. temporally varying buoyancy forcing, which may be more important in the case of the Black Sea, as compared to other possible forms of external forcing.

Spitz and Nof (1991) indicate that a barotropic boundary current would be forced to separate from the coast when it encounters a large step with the depth increasing downstream. In fact, barotropic flows impinging on a step topography can be expected to generate large amplitude baroclinic motions (e.g. Cushman-Roisin and O'Brien, 1987). Häkkinen (1987) illustrated that interaction of baroclinic and barotropic components of a boundary current with the canyon or ridge topographies creates oscillatory motions. The role of bottom topographic features was found to magnify the baroclinic instability in the case studied by Ikeda et al. (1989). Haidvogel et al. (1991) and Hoffmann et al. (1991) found offshore filaments generated by the interaction of a boundary current with topographic variations, and the evolving filaments led to self-advecting dipole eddies detached from the coastal region during later stages of development.

Leaman and Molinari (1987) studied the effects of a linearly widening shelf and found that this situation can lead to vertically sheared flows perpendicular to the coast, resulting in flow separation as in the case of the west Anatolian boundary current separating from the coast at C. Kerempe where the flow encounters a widening shelf topography. The Boyer and Chen (1987) experiments illustrate eddy shedding and separated flows downstream of headlands. A secondary factor leading to flow separation could be the change in the angle of the coastline near C. Kerempe.

Note that the cyclonic circulation of the Black Sea inferred from Figs. 3–7 correspond to a period when the Danube discharge is maximum (Fig. 2). The early summer bloom indicated rapid changes in the spatial distribution of species, with

Fig. 4. Coastal Zone Color Scanner (CZCS) satellite images on June 15, 1980. The images represent the atmospherically corrected (a) channel 1 (443 nm), (b) channel 3 (550 nm).

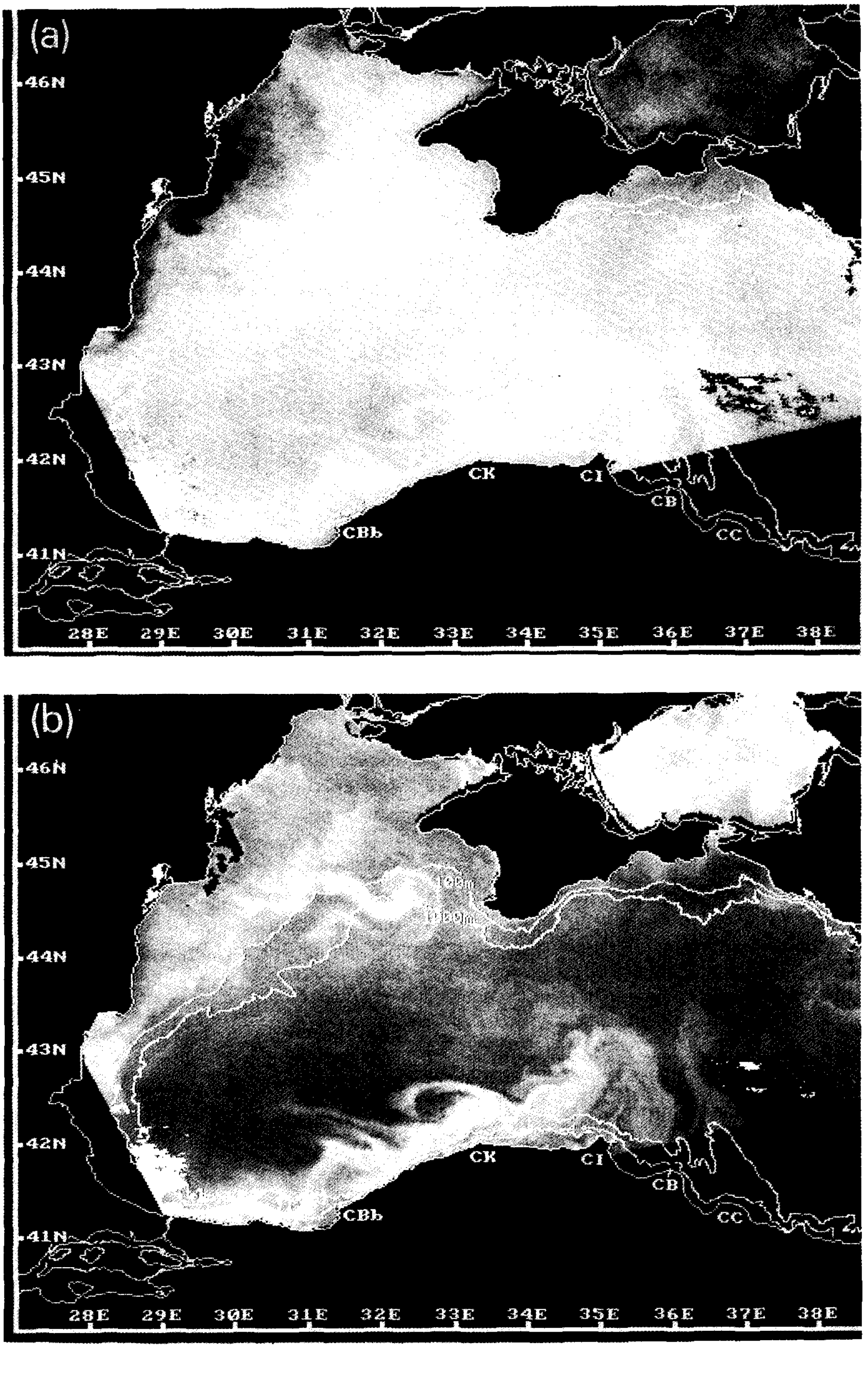
(a)
46N
45N
44N
43N
42N
41N
CK
CI
CB
CC
CBb
28E 29E 30E 31E 32E 33E 34E 35E 36E 37E 38E
(b)
46N
45N
44N
43N
42N
41N
100m
1000m
CK
CI
CB
CC
CBb
28E 29E 30E 31E 32E 33E 34E 35E 36E 37E 38E

E. huxleyi dominating the western basin excluding the near field of the Danube delta.

Based on sediment trap deployments, Hay and Honjo (1989) studied the vertical flux of particles. At a site 40 km offshore from Amasra (west of C. Kerempe), *E. huxleyi* blooms were detected in the summer, autumn and early winter, in contrast to the traps further offshore (80 km offshore from the Sakarya Canyon), where more than half of the annual particle flux was deposited during short (one month) periods of spring/summer blooms.

In Figs. 3–7, initially much of the interior and the eastern basin have considerably smaller pigment and particulate concentrations. The spreading pattern of production displayed in the figures implies that the eutrophication must have started near the Danube, and proceeded south along the shelf, finally reaching the interior via cross-frontal turbulent exchanges during the early part of the last decade. It is suspected that this pattern has been significantly altered in the recent years, leading to a recent decrease in the optical transparency of the surface waters even at the central regions of the Black Sea (Eremeev et al., 1992), implying intense basin-wide phytoplankton blooms, confirmed by some of our recent data.

4.2. Filaments and dipole vortices

A massive plankton bloom originating from the northwestern shelf can be identified in Fig. 8, 9. High spectral reflectance is obtained in all visible CZCS channels indicating an *Emiliana huxleyi* bloom. The bloom extends south from the shelf, reaching the middle of the basin, although the minimum river discharges are expected during this season (Sur et al., 1994) suggest northerly winds or a bloom independent of the size of the river plume. Six days later, the plankton bloom in the northeastern sector is found to be larger in size, and more complicated in texture (Fig. 9a).

Riverine influence is also recognized in the CZCS images of October 7, 1980 originating from the Kızılırmak and Yeşilırmak rivers, and from other small streams along the central Anatolian coast. They are observed to bend eastwards as a result of the boundary current system, and to form small eddies in the adjoining bays (east of Cape İnce, Cape Bafra and Cape Çalti). The pigment signal of the plumes (Fig. 8b), partly associated with river-borne organics (e.g. plant debris and yellow substance), is typically smaller than the particulate signal (Fig. 8a).

In Fig. 9a (October 13, 1980), a mushroom eddy is visible offshore of the mouth of the Kızılırmak river at Cape Bafra. In the enlarged image of the Anatolian coast (Fig. 9b), unique features can be observed. The asymmetric spiral pattern of the tracer field trapped in the doublet, and the pattern of streamers surrounding the eddies are remarkably similar to the patterns generated in laboratory simulations.

Fedorov and Ginsburg (1989) and Fedorov et al. (1989) view dipole structures to be the universal reaction of a rotating fluid to applied impulses. The momentum impulse could result from local dynamical instabilities, local winds, or river discharges. During initial development, the dipoles are often asymmetric or immature, but when a surface tracer is present (for example, sea surface temperature, biota, sediments), the basic surface signature of a dipole eddy is a mushroom-like pattern. Dipole eddies resulting from instabilities of boundary currents are also common (e.g. Griffiths and Linden, 1981).

The tracer pattern in Fig. 9b appears mainly related to river sediments, as well as some pigments carried by river water. The mushroom feature consists of equal sized cyclonic and anticyclonic eddies, extending 60 km offshore, and connected to the coast by the river plume which seems to follow the local canyon topography of the Arhangelsky Ridge. This topographic control

Fig. 5. Coastal Zone Color Scanner (CZCS) satellite images on June 22, 1980. The images represent the atmospherically corrected (a) channel 1 (443 nm), (b) channel 3 (550 nm).

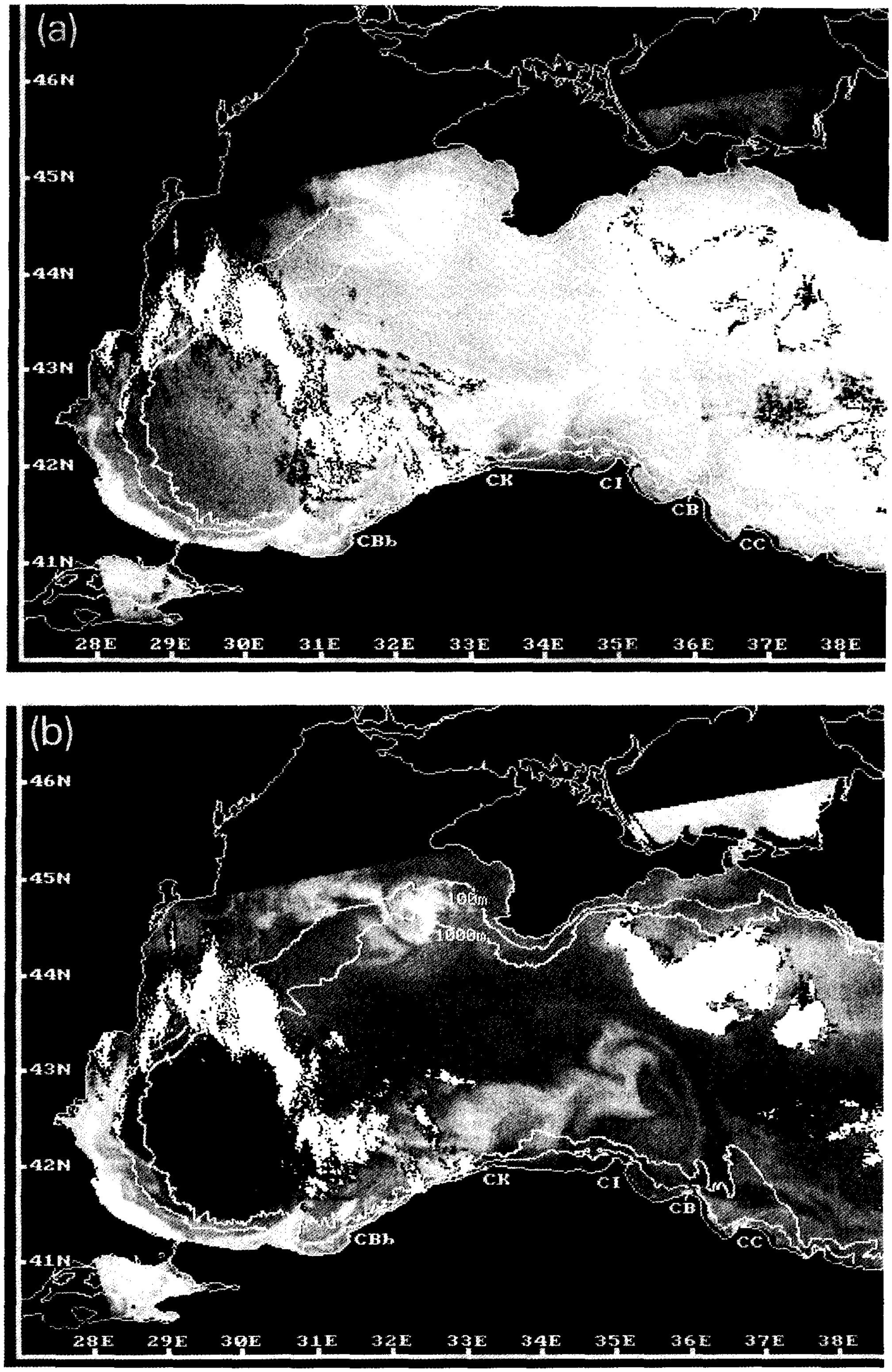
(a)
46N
45N
44N
43N
42N
41N
28E 29E 30E 31E 32E 33E 34E 35E 36E 37E 38E
CK
CI
CB
CC
CBb
(b)
46N
45N
44N
43N
42N
41N
100m
1000m
28E 29E 30E 31E 32E 33E 34E 35E 36E 37E 38E
CK
CI
CB
CC
CBb

is surprising despite the fact that the flow is expected to be confined in the surface layers. The dipole vortex could be an unstable feature generated by a pulse of momentum imparted by local winds, the river plume itself, or instabilities of the boundary current. A number of filaments extending offshore from the coast near C. Kerempe suggest instability of the boundary current.

4.3. Winter convection on the western shelf

An infra-red (AVHRR) image (Fig. 10a) during February 1990 indicates cold water with uniform temperatures along the entire western continental shelf on February 27, 1990. This well mixed water has a uniform temperature of 6.5°C and salinity < 18 in the upper 30–40 m along the southern coast (Fig. 10b, c). The boundary of the cold water follows a constant depth contour between 50 and 100 m along the entire western shelf with a gradually decreasing width towards the south; it then becomes much narrower along the shallow inner part (< 100 m) of the Sakarya Canyon (Fig. 10a), and upon reaching the concave coastline east of the Canyon it expands near C. Baba where the shallow region suddenly ends. The temperature structure displayed in Fig. 10a and b near C. Baba is very similar to a shock; the narrow band of cold water suddenly expands and continues to flow along the coast with a sudden increase in width.

In Fig. 10a, we also identify warm water along the continental slope offshore of the shelf waters, which gradually disappears by frontal mixing with the cold shelf water on the western and southern coasts. This gradual blending of the cold and warm waters proceed along the coast from west of Crimea upto near C. Baba. The tongue of cold water diminishes towards east after its separation from the coast until C. İnce, as it is evident in Fig. 10b.

Phytoplankton data during February 1990 indicated an intense bloom along the Turkish coast within the cold water area of the satellite image. The diatom *Chaetoceros sp.* was dominant in the same area, having an abundance of more than 91% with respect to the total phytoplankton (sizes > 55 μm). The abundance increased in the coastal area adjacent to C. Baba (the total number of individuals increased logarithmically to $> 10^6$ cells/l), and decreased gradually towards the east. There was a parallel increase in number of species near the coast (54 coastal species versus 10 offshore species) (Uysal, 1993). It is not clear whether this high abundance of dominant phytoplankton species was linked with local production resulting from nutrients supplied by the cold water vein or nutrients entrained from the deep water, or the transport of plankton from the north-west shelf.

A similar structure of winter convection along the western shelf was evident on AVHRR images obtained during 1994. In the beginning of February (Fig. 11a), the western shelf was covered by cold water with a strong front following the 50 m depth contour from Crimea to the Rumelian coast. This band of cold water widened and reached the Sakarya Canyon within 20 days (Fig. 11b), indicating small-scale mixing along the front. Filaments and dipole eddies were initiated some days later (Fig. 11c)along the southern coast and near the canyon.

4.4. Upwelling along the Anatolian coast

A review of satellite data indicates recurring upwelling events along the Turkish coast between Cape Baba and Cape İnce, starting in early summer and lasting until early fall (Sur et al., 1994). The exact mechanism leading to upwelling largely remains unexplained. However, Sur et al. (1994) suggest that the time dependent motions interact-

Fig. 6. Coastal Zone Color Scanner (CZCS) satellite images on June 25, 1980. The images represent the atmospherically corrected (a) channel 1 (443 nm), (b) channel 3 (550 nm).

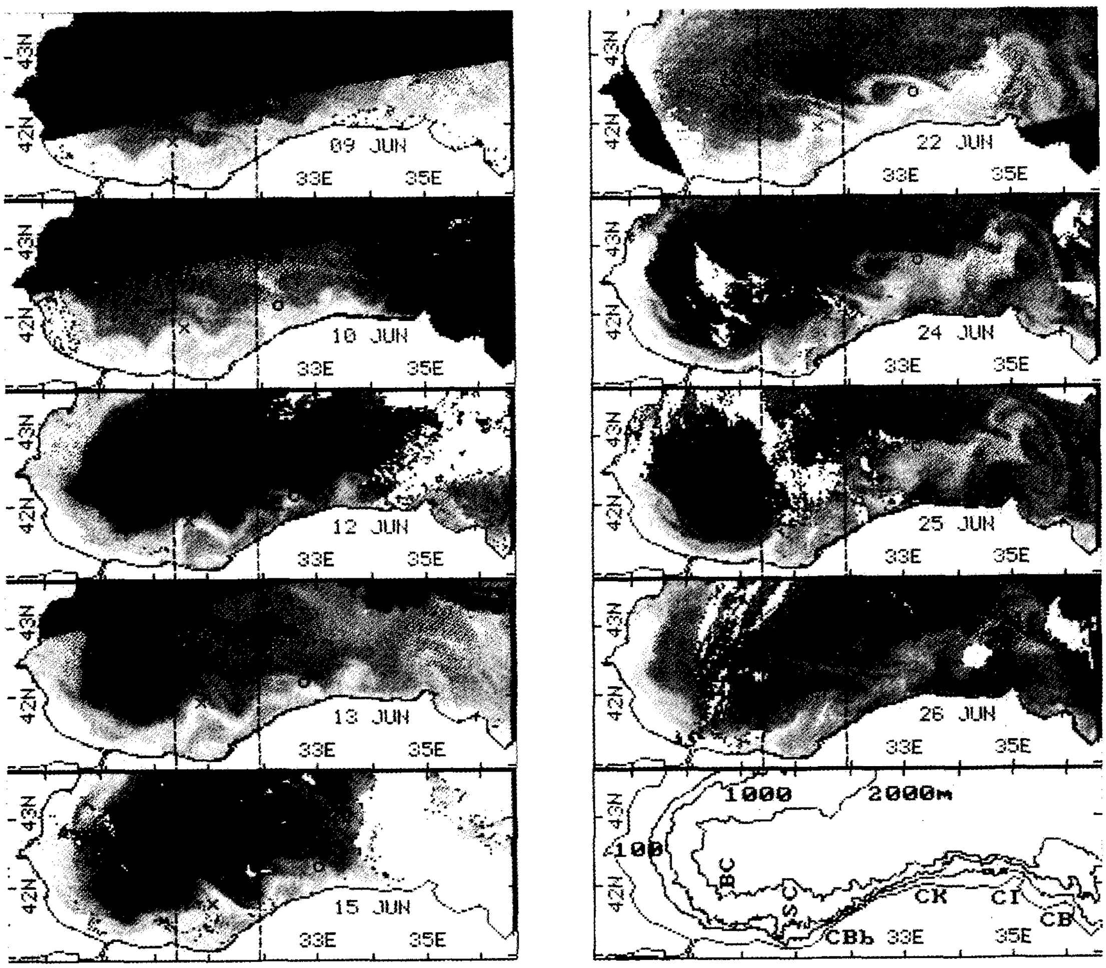

Fig. 7. A sequence of CZCS channel 3 (550 nm) images for the period 9 June–26 June 1980. Abbreviations used: *SB*: Bosphorus Canyon, *SC*: Sakarya Canyon, *CBb*: Cape Baba, *CK*: Cape Kerempe, *CI*: Cape İnce, *CB*: Cape Bafra.

ing with the coastline geometry and continental slope bathymetry appear capable of creating upwelling events in which surface divergence within the thin mixed layer can induce upward penetration of the underlying Cold Intermediate Water. Similar transient upwelling along fronts and unstable current systems are known to exist elsewhere (e.g. Millot, 1991; Beckers and Nihoul, 1992).

An example is provided by the upwelling event in July 1992 (Fig. 12a, b) resulting in surface temperatures as low as 12°C along the Anatolian coast. Measurements during this detailed survey (Niermann et al., 1993) indicated that only very

Fig. 8. Coastal Zone Color Scanner (CZCS) satellite images on October 7, 1980. The images represent the atmospherically corrected (a) channel 3 (550 nm) and (b) the pigment concentration.

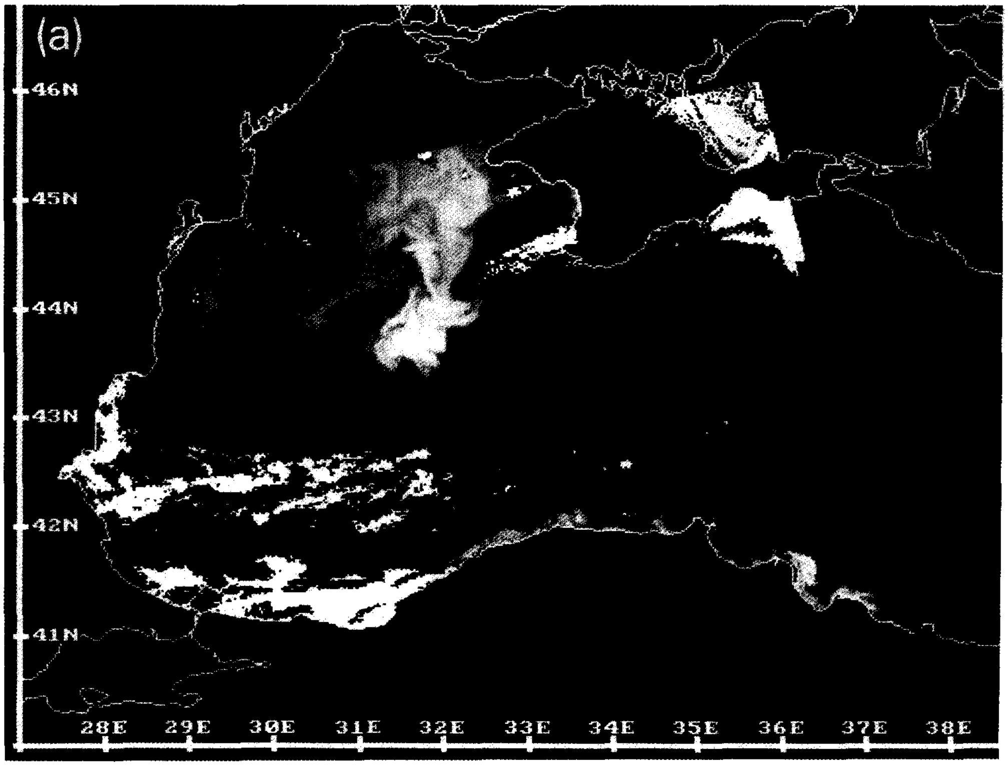
(a)
46N
45N
44N
43N
42N
41N
28E
29E
30E
31E
32E
33E
34E
35E
36E
37E
38E

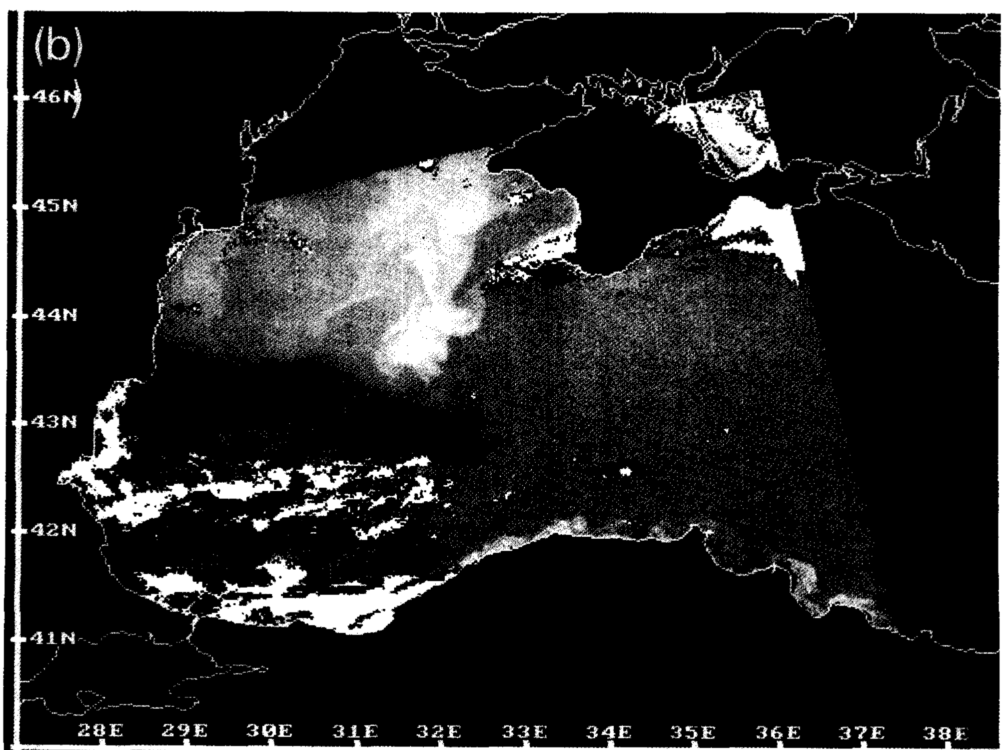
(b)
46N
45N
44N
43N
42N
41N
28E
29E
30E
31E
32E
33E
34E
35E
36E
37E
38E

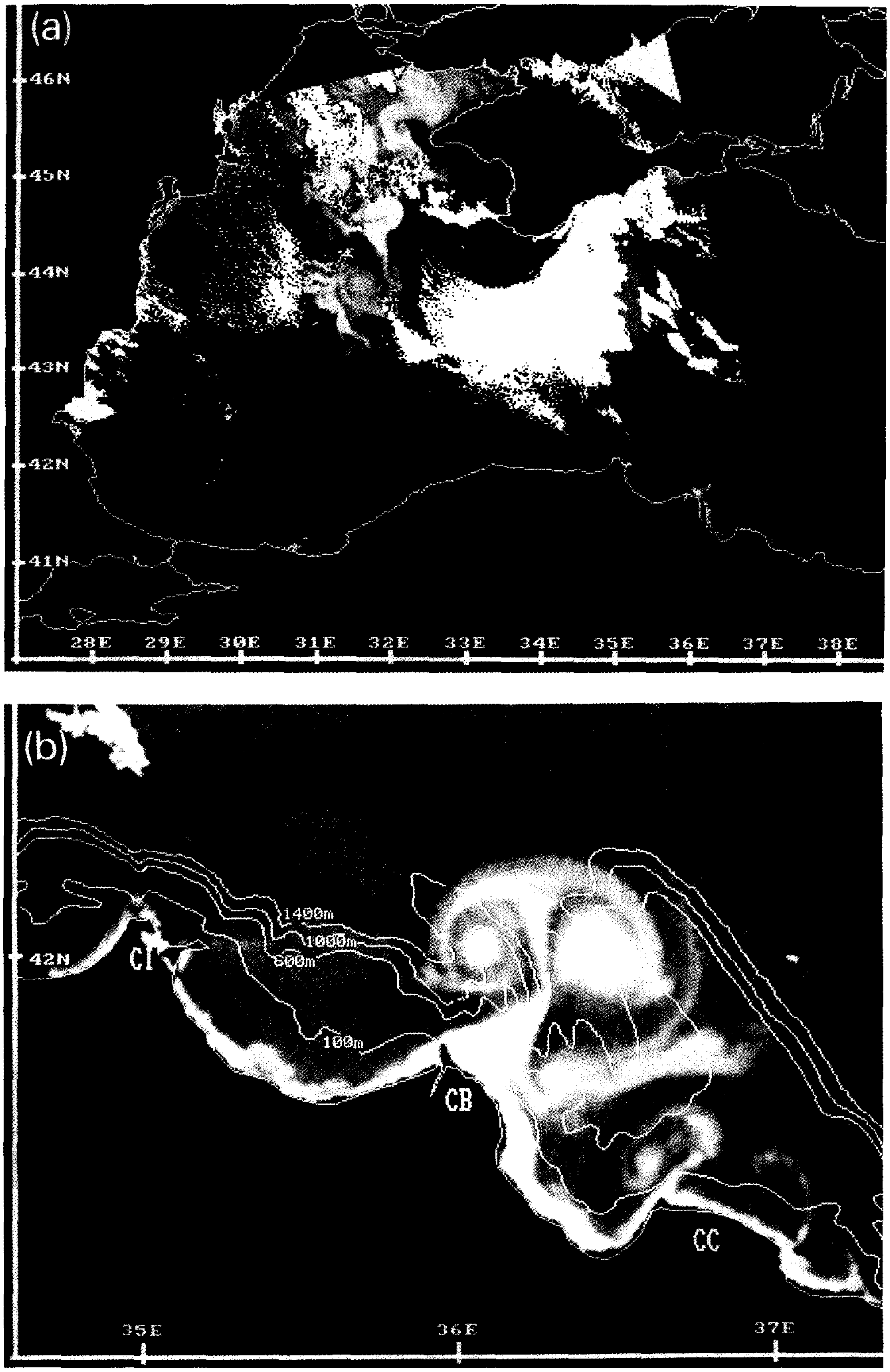
(a)
46N
45N
44N
43N
42N
41N
28E
29E
30E
31E
32E
33E
34E
35E
36E
37E
38E
(b)
1400m
1000m
600m
100m
42N
CI
CB
CC
35E
36E
37E

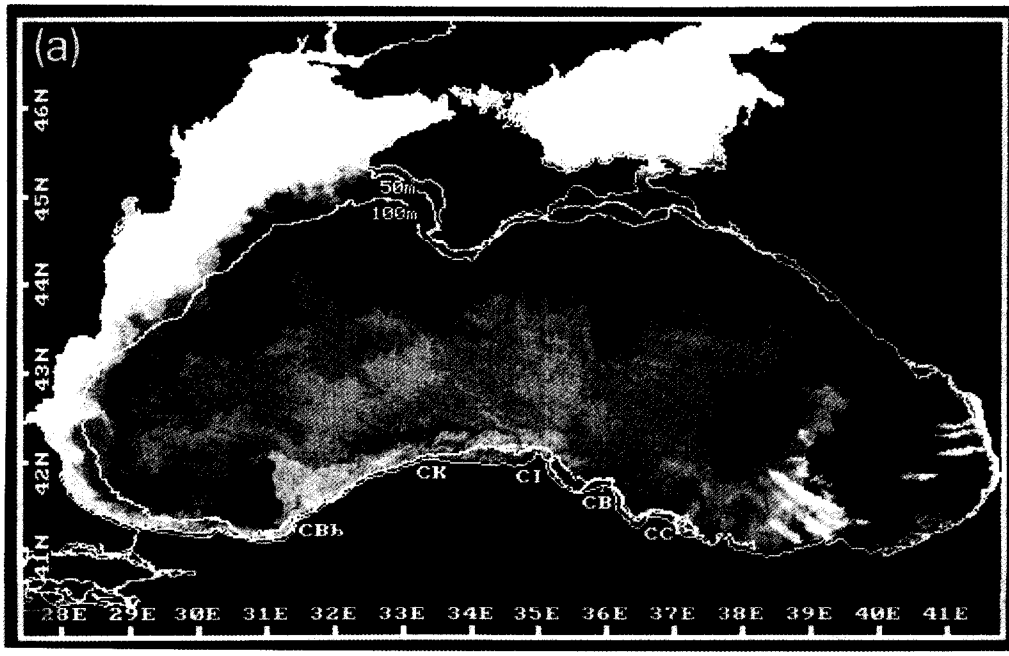

FEBRUARY 1990

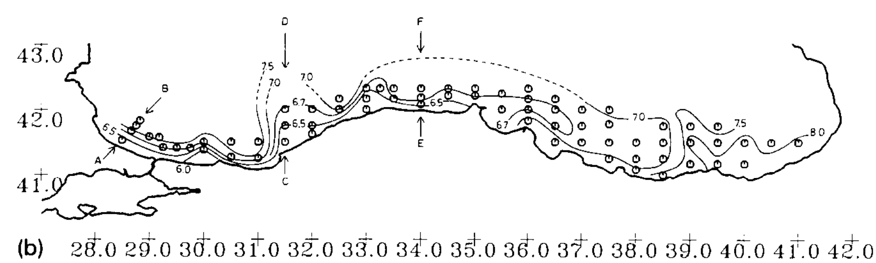

Fig. 10. (a) Advanced Very High Resolution Radiometer (AVHRR) satellite image on February 27, 1990 (NOAA-10 Channel 4), (b) Surface temperature distribution and (c) cross-shore hydrographic sections depicted by arrows in (b), during the February 1990 cruise of the R/V BİLİM.

few eggs and larvae of anchovy were present in the cold water patch of Fig. 12, although they were abundant elsewhere. At the same location, both phyto- and zoo-plankton were present near the surface; in fact, some yet unidentified species of phytoplankton and some copepods (especially

Fig. 9. (a) Coastal Zone Color Scanner (CZCS) satellite image on October 13, 1980 and (b) its enlarged form for a dipole eddy near the mouth of the Kızılırmak river. Both images are the atmospherically corrected channel 3 (550 nm) of the CZCS.

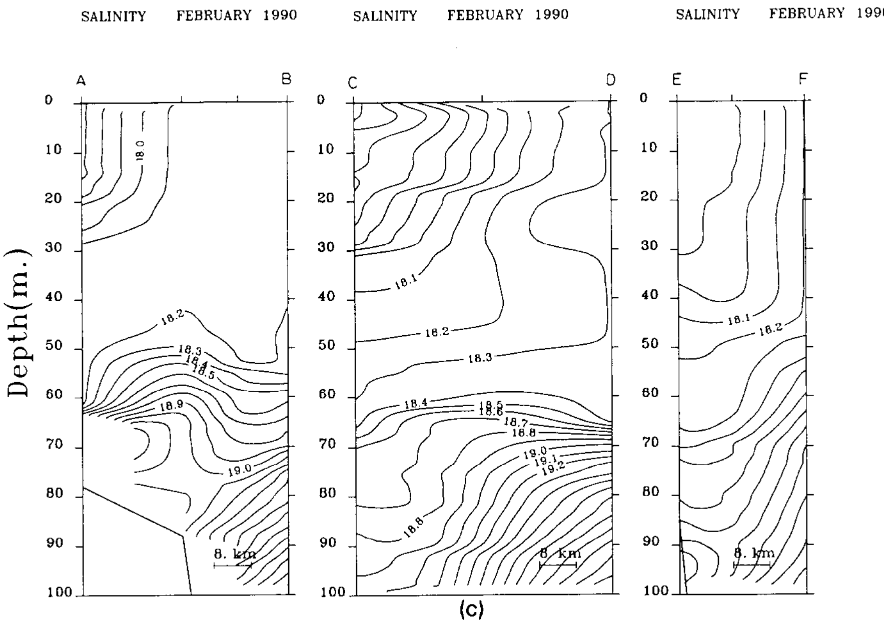

Fig. 10. (continued).

the cold water species *P. elongatus*) were more abundant in the cold water patch as compared to the surroundings. The decreased abundance of ichthyoplankton, despite a presence of phyto- and zoo-plankton, in the cold water patch seems to suggest that the spawning of anchovy was suppressed by the cold, upwelled waters (Sur et al., 1994).

It is interesting that a similar situation was present during a survey in July 1957 (Einarsson and Gürtürk, 1960; Niermann et al., 1993), but could only be recognized in the light of the recent interpretation of satellite and in-situ data (Sur et al., 1994). In this case, the upwelling region extended from Cape Baba to Cape İnce region, with a cold spot with temperatures as low as 11.6°C (at 10 m depth) in the same location as the 1992 upwelling. A total lack of anchovy eggs was similarly observed in the upwelling region (Niermann et al., 1993).

4.5. Coherent eddies and synoptic / mesoscale turbulent structures

In addition to the above, coherent eddies and turbulent features are quite common in the Black Sea. Often the coherent structures emerge, decay, or change form and position with fascinating rapidity.

A very turbulent flow pattern with embedded coherent features was observed in April 1993. The sea surface dynamical topography calculated from hydrographic and ADCP current data (Güngör, 1994) during this period only showed the coarse meso-scale and synoptic features, including the boundary current and the series of anticyclonic eddies to the left of the Crimean Peninsula and along the western continental shelf, on the periphery of the cyclonic central region (Fig. 13a). The ADCP horizontal current vectors at 10 m (Fig. 13b) coincided with these features and verified the swiftly meandering boundary current with speed of up to 100 cm/s along the continental slope region, and relatively weaker flows in the north-west shelf and in the central parts of the sea (5–15 cm/s). The nearest cloud free AVHRR image, on April 19, 1993 (Fig. 13c) shows the boundary current and an elliptical shaped anticyclonic eddy southwest of Sevastopol, with a size of 100 km, and centered at 44.5°N, 32.1°E. This eddy has a cold core which has a temperature anomaly of −1.2°C at its center. We believe the cold anomaly results from the three-layer structure of the eddy, with a seasonal thermocline separating the shallow mixed layer from the underlying cold intermediate water (CIW), and a much weaker permanent thermocline coinciding with the main pycnocline underlying the CIW. Despite the convergence created by the anticyclone, such a structure could result in surfacing of the CIW at the center.

As a result of the convective cooling in the preceding winter, the north-west shelf is colder (by 1.5–2.0°C) than the boundary current region along the continental slope. Near the western coast, the Danube waters are well traced, by their characteristics which are warmer (by about 1.5°C) as compared to the shelf water. River plumes discharging from the three delta tributaries of the Danube (Kilija, Sulina and St. George) are clearly distinguished, which then form a narrow band of warm water along the coast. The cold northwest shelf water becomes entrained between the warm nearshore and continental slope waters as it proceeds south along the coast. Along the south coast, a warm easterly current transports these

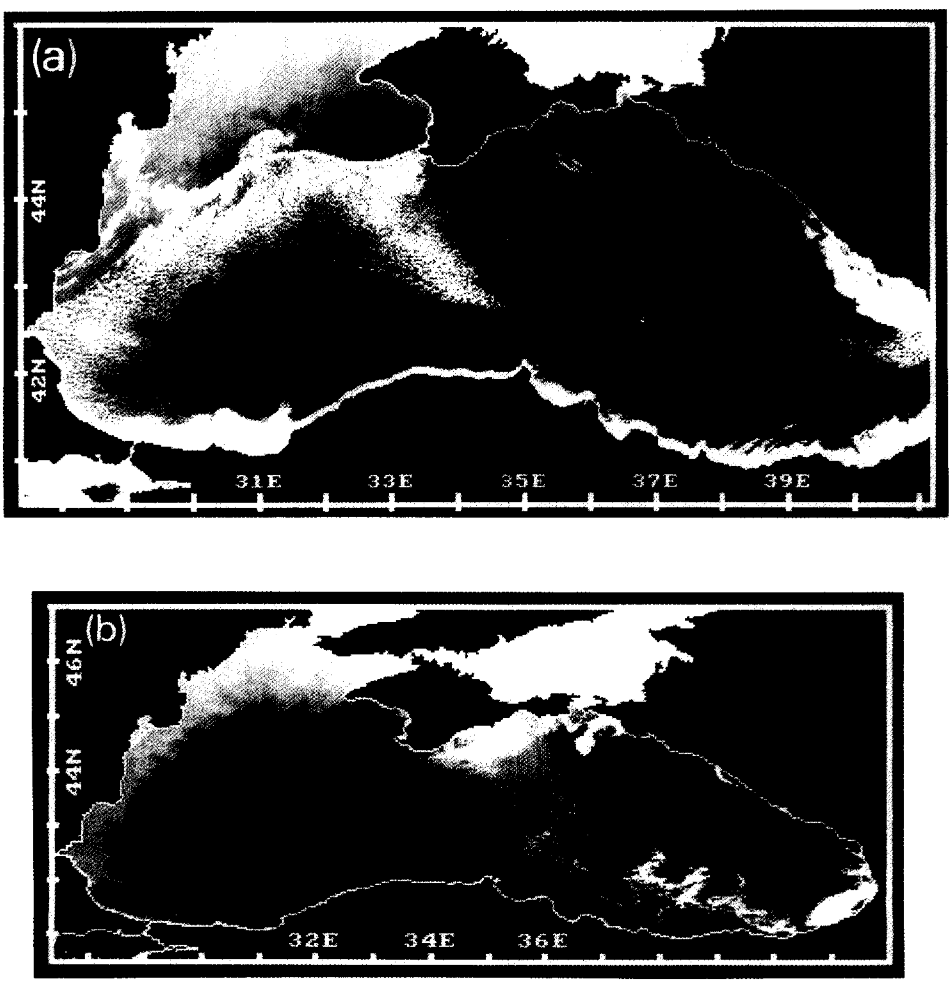

Fig. 11. AVHRR-Infrared satellite image on (a, b) February 9, 28, 1994 and (c) March 16, 1994.

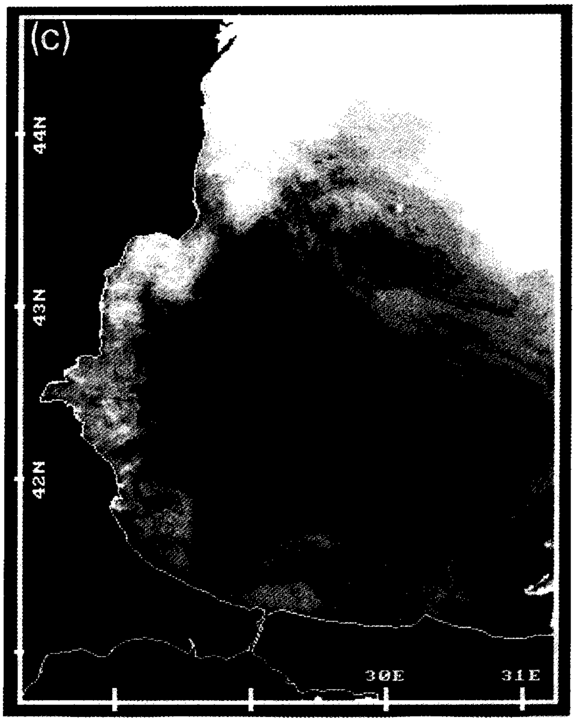

Fig. 11. (continued).

bands of alternating temperature signatures (Fig. 13c, d). A small anticyclonic eddy of size 40 km centered at 42.5N, 31.7E is remarkable in that it too has a cold center with a temperature anomaly of about −6°C, and it is connected to the warm boundary current with a filament. Note that this small eddy is also captured in the ADCP measurements (Fig. 13b).

AVHRR images in June 1994 show coherent anticyclonic eddies along the continental slope, and transient upwelling structures on the western shelf and along the other coasts all around the basin (Fig. 14). Similar cases of upwelling were reported earlier by Tolmazin (1985), who attributed them to the surfacing of cool bottom water in response to southwesterly winds in the months of June and July, when the mixed layer is relatively thin (5–10 m). On the other hand, it is hard to explain upwelling simultaneously occurring at preferred locations all around the basin and at the center of the Sevastopol anticyclonic eddy, by favorable wind directions alone. It is evident that the closed basin configuration of the Black Sea (continuity constraints) play a leading role in the pattern of transient coastal upwelling. The upwelling along the western half of the south coast has been documented by Sur et al. (1994). A sequence of AVHRR images during June 1994 (not shown) emphasize the transience of the upwelling structures: while the upwelling along the northwestern and southern coasts first increases then subsides during this period, the upwelling along the western coast of Crimea is observed to increase continuously with time.

The meandering of the boundary current occasionally goes into a high amplitude mode along the northeastern (Caucasian) coast. Sur et al. (1994) observed such meanders in September 1991, downstream of the large Batumi anticyclone, a semi-permanent feature trapped in the southeast corner of the Black Sea. In that case the meanders grew until they made large excursions into the interior (almost reaching the south coast) until when they developed turbulent structures. Similar developments are observed in AVHRR images of 1994, in which an intense coherent eddy along the Caucasian coast off Sukhumi and another warm anomaly off Novorossiysk (Fig. 11a), constituting the elements of a large meander mode finally broke up into warm turbulent structures (Fig. 11b) along the Caucasian coast, with excursions reaching well into the interior, only 20 days later than the first image. It is not clear where the initial coherent eddy in Fig. 11a came from, because of a lack of good images in winter, but it is most likely that it originated from the Batumi eddy, traces of which can be seen in the residual warm water patches along the southeast coast in the same figure.

5. Conclusions

CZCS derived pigment and particulate fields together with infra-red images provide a good opportunity to study the meso-scale circulation features and the distributions of competing species of phytoplankton, leading to a better understanding of the progression of eutrophication in the Black Sea.

It is seen that the materials originating from lateral sources are transported by the boundary current flowing along the continental slope topography, and are later spread along the coast

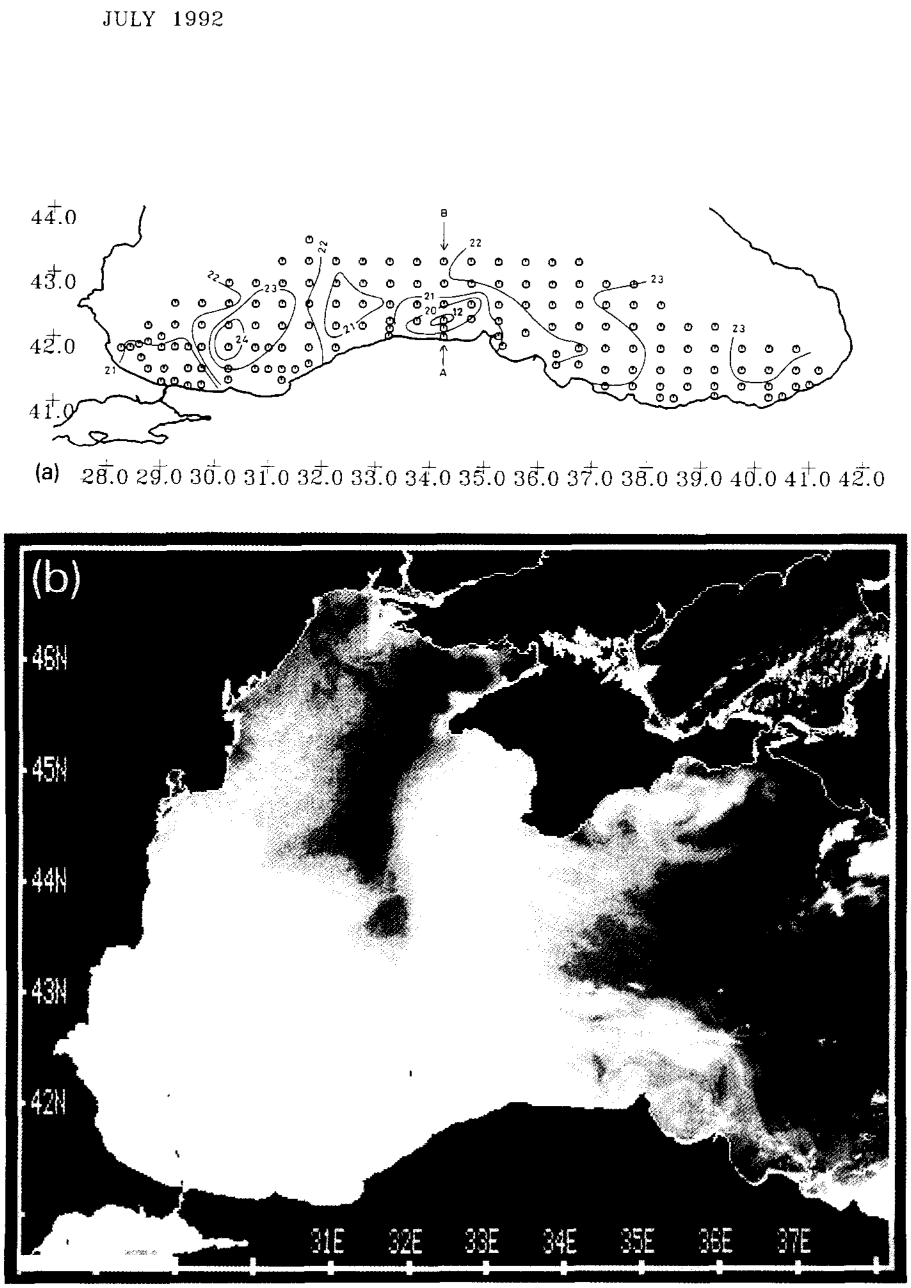

Fig. 12. (a) Surface temperature (°C) during the July 1992 cruise of the R/V *BILIM* and (b) AVHRR-Infrared satellite image on July 28, 1992 (NOAA-11 Channel 4).

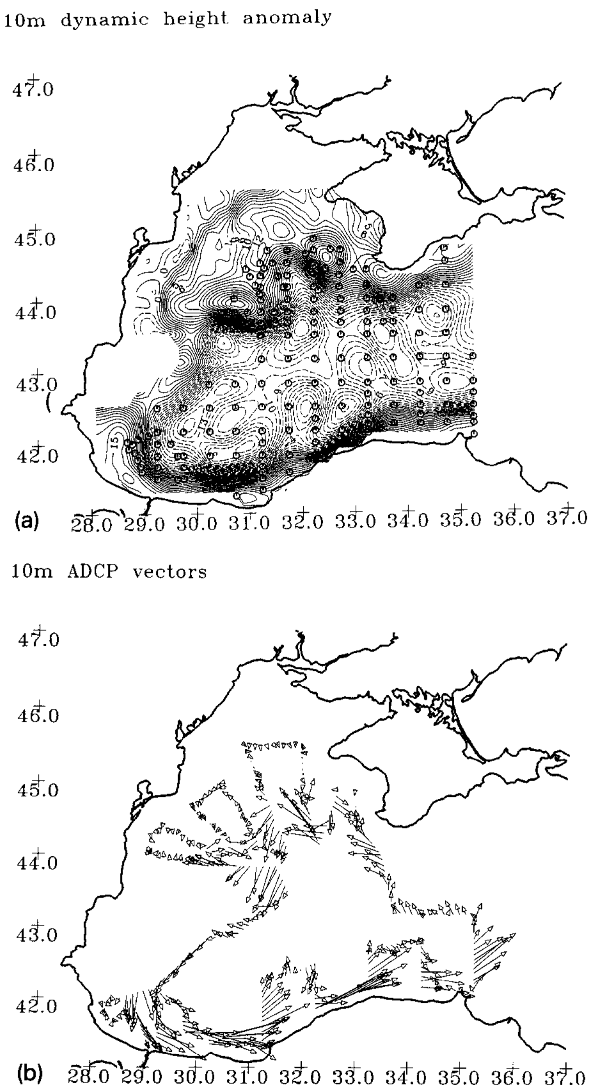

Fig. 13. (a) Surface dynamic topography (cm), referenced to 500 m during the April 1993 cruise of the R/V *BİLİM*, (b) ADCP current measurements at 10 m depth, and (c, d) infrared AVHRR images in April 19, 23, 1993 (NOAA-11 Channel 4).

and across the frontal region by turbulent motions, which either result from instability mechanisms or are initiated by interactions with the sharp along-shore topographic variations. It is also evident that the transport and vertical motions along the coast is influenced by flow separation resulting from the changes in shelf topography or headlands.

Upwelling is another phenomenon with rapidly varying distribution along particular stretches of the weastern coast in summer. Although the basic mechanism leading to upwelling remain largely unexplained, it is suggested that the interaction of the currents with the coastline geometry and bottom topography (Sur et al., 1994), as well as surface divergences within the shallow mixed layer overtopping CIW could induce upwelling without need for wind forcing.

Coherent anticyclonic eddies and large amplitude meanders of the coherent jet flow along the basin periphery display rapid evolution, in terms of their development and decay into turbulence. These features develop significant transport around the basin and between the coastal and open sea. The advection of materials along the periphery of the basin and the cross-shelf transports created along the boundary current are important for the spreading of productivity and the subsequent basin-scale eutrophication processes, and sets the time and space scales of a succession of plankton blooms and their transformation into higher trophic levels. It is also recognized that these circulation features are important for the migration/spawning behavior of the mainly pelagic fish stocks of the Black Sea.

Acknowledgements

This study was made possible through the TU-FISHERIES, the TU-BLACK SEA Projects of the NATO Science for Stability Program, and a NATO Linkage Grant between the IMS-METU Erdenli, and MHI, Sevastopol; and was partially supported by the Turkish Scientific and Technical Research Council (TUBİTAK).

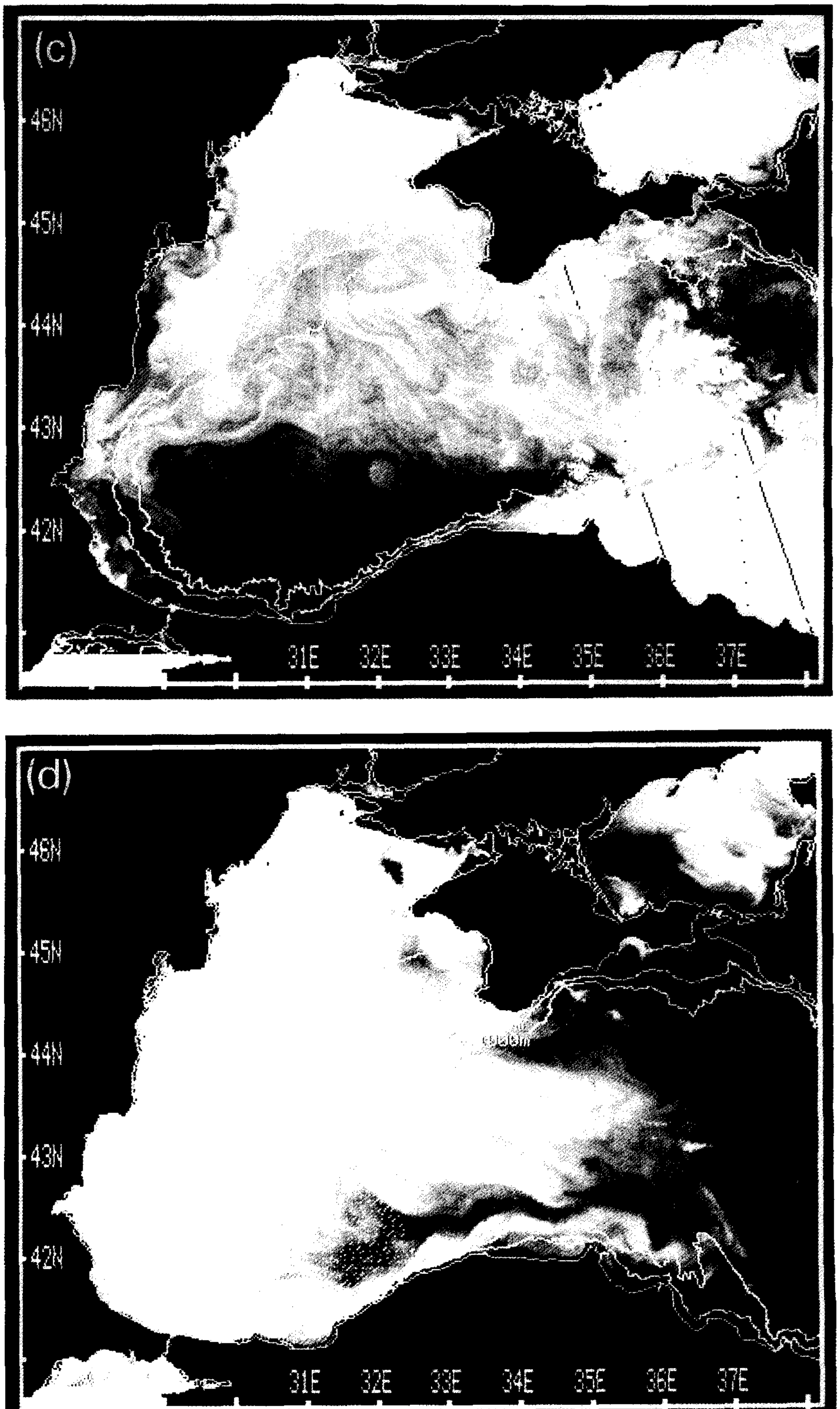

Fig. 13. (continued).

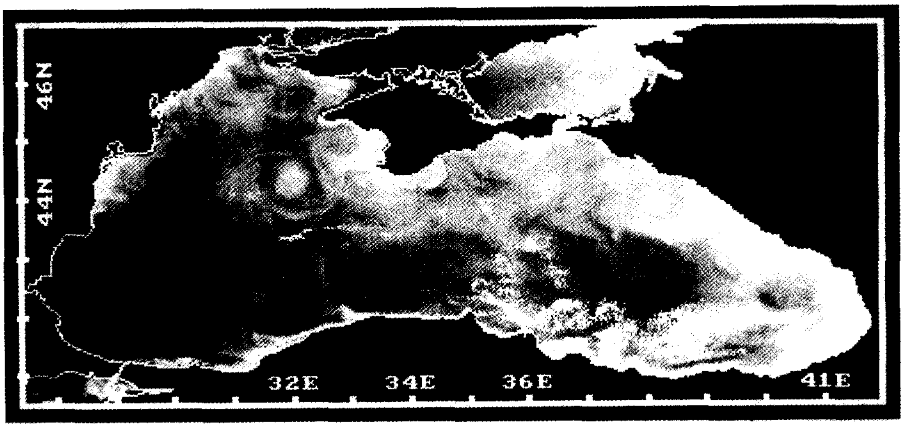

Fig. 14. AVHRR-Infrared satellite image on June 26, 1994.

References

Acara, A., 1958. Fluctuation of the Surface Water Temperature and Salinity of the Bosphorus. Rapp. P.-V. Reunions C.I.E.S.M.M., 15(3): 255-258.

Ahlnäs, K., Royer, T.C. and George, T.H., 1987. Multiple dipole eddies in the Alaska coastal current detected with Landsat thematic mapper data. J. Geophys. Res., 92: 13,041-13,047.

Artüz, M.I. and Uğuz, H.C., 1976. Daily Observations on the Hydrographic Conditions of the Bosphorus During the Period of 1967-1970. Publ. Hydrobiol. Res. Inst. Fac. Science, Univ. İstanbul, 16, 35 pp. (in Turkish)

Beckers, J.M. and Nihoul, J.C.J., 1992. Model of the Algerian current's instability. J. Mar. Syst., 3: 441-451.

Benli, H., 1987. Investigation of plankton distribution in the southern Black Sea and its effects on particle flux. In: E.T. Degens, E. İzdar and S. Honjo (Editors), Particle Flux in the Ocean. Mitt. Geol.-Paleontol. Inst., Univ. Hamburg, 62: 77-87.

Bologa, A.S., 1986. Planktonic primary productivity of the Black Sea: A review. Thalassia Jugosl., 22: 1-22.

Bologo, A.S., Bodeanu, N., Petron, A., Tiganus, V. and Zaitsev, Yu.P., 1995. Major modifications of the Black Sea benthic and planktonic biota in the last three decades. Bull. Inst. Océanogr. Monoco, Numéro Special, 15: 85-110.

Bondar, C., 1989. Trends in the evolution of the mean Black Sea level. Meteorol. Hydrol. (Romania), 19: 23-28.

Boyer, D.L. and Chen, R., 1987. On the formation and shedding of vortices from side-wall mounted obstacles in rotating systems. Dyn. Atmos. Oceans, 11: 59-86.

Chao, S-Y., 1990. Instabilities of fronts over a continental margin. J. Geophys. Res., 95: 3199-3211.

Cushman-Roisin, B. and O'Brien, J.J., 1987. The influence of bottom topography on baroclinic transports. J. Phys. Oceanogr., 13: 1600-1611.

Deschamps, P.Y. and Frouin, R., 1984. Large diurnal heating of the sea surface observed by the HCMR experiment. J. Phys. Oceanogr., 14: 177-184.

Einarsson, H. and Gürtürk, N., 1960. Abundance and distribution of eggs and larvae of the anchovy (*Engraulis encrasicholus ponticus*) in the Black Sea (Results of the pektaş expedition). Hydrobiol. Res. Inst. Fac. Sci., Univ. İstanbul, Series B, 5(1-2): 71-94 + 2 plates.

Eremeev, V.N., Vladimirov, V.L. and Krasheninnikov, B.N., 1992. Long-term variability of the Black Sea water transparency. In: Hydrophysical and Hydrochemical Studies of the Black Sea. Mar. Hydrophys. Inst., Ukraine Acad. Sci., Sevastopol, pp. 28-30.

Fedorov, K.N. and Ginsburg, A.I., 1989. Mushroom-like currents (vortex dipoles); one of the most widespread forms of non-stationary coherent motions in the ocean. In: J.C.J. Nihoul and B.M. Jamart (Editors), Mesoscale Synoptic Coherent Structures in Geophysical Turbulence. Elsevier, Amsterdam, pp. 1-14.

Fedorov, K.N., Ginsburg, A.I. and Kostianoy A., 1989. Modelling of "mushroom-like" currents (vortex dipoles) in a laboratory tank with rotating homogenous and stratified fluids. In: J.C.J. Nihoul and B.M. Jamart (Editors), Mesoscale/Synoptic Coherent Structures in Geophysical Turbulence. Elsevier, Amsterdam, pp. 15-24.

Gordon, H.R., Clark, D.K., Brown, J.W., Brown, O.B., Evans, R.H. and Broenkow, W.W., 1983. Phytoplankton pigment concentrations in the middle Atlantic Bight: comparison of ship determinations and CZCS estimates. Appl. Opt., 22(1): 20-36.

Güngör, H., 1994. Multivariate Objective Analyses of ADCP and CTD Measurements Applied to the Circulation of the Laventine Sea and Black Sea. M.S. Thesis, Institute of Marine Sciences, Middle East Technical University.

Griffiths, R.W. and Linden, P.F., 1981. The stability of buoyancy-driven coastal currents. Dyn. Atmos. Oceans, 5: 281-306.

Haidvogel, D., Beckmann, A. and Hedström, K., 1991. Dynamical simulations of filament formation and evolution in the coastal transition zone. J. Geophys. Res., 96: 15,017–15,040.

Häkkinen, S., 1987. Feedback between ice flow, barotropic flow and baroclinic flow in the presence of bottom topography. J. Geophys. Res., 92: 3807–3820.

Hay, B.J. and Honjo, S., 1989. Particle Deposition in the Present and Holocene Black Sea. Oceanography, 2: 26–31.

Hay, B.J., Honjo, S., Kempe, S., Itekkot, V.A., Degens, E.T., Konuk, T. and İzdar, E., 1990. Interannual variability in particle flux in the southwestern Black Sea. Deep-Sea Res., 37: 911–928.

Hay, B.J., Arthur, M.A., Dean, W.E. and Neff, E.D., 1991. Sediment deposition in the Late Holocene abyssal black sea: Terrigenous and biogenic matter. Deep-Sea Res., 38 (Suppl.): S711–S723.

Hoffmann, E.E., Hedström, K., Moisan, J., Haidvogel, D. and Mackas, D.L., 1991. Use of simulated drifter tracks to investigate general transport patterns and residence times in the coastal transition zone. J. Geophys. Res., 96: 15,041–15,052.

Holligan, P.M., Viollier, M., Harbour, D.S., Camus, P. and Champagne-Philippe, M., 1983. Satellite and ship studies of coccolithophore production along a continental shelf edge. Nature, 304: 339–342 and 667–765.

Ikeda, M., Mysak, L.A. and Emery, W.J., 1984. Observation and modelling of satellite-sensed meanders and eddies off Vancouver Island. J. Phys. Oceanogr., 14: 3–21.

Ikeda, M., Johanessen, J.A., Lygre, K. and Sandven, S., 1989. A process study of mesoscale meanders and eddies in the Norwegian coastal current. J. Phys. Oceanogr., 19: 20–35.

Koblentz-Mishke, O.J., Volkovinsky, V.V. and Kabanova, J.G., 1970. Plankton primary production of the world ocean. In: W.S. Wooster (Editor), Scientific Exploration of the South Pacific. Natl. Acad. Sci., Washington, pp. 183–193.

Latun, V.S., 1990. Anticyclonic eddies in the Black Sea in summer 1984. Sov. J. Phys. Oceanogr., 1: 279–286 (in Russian).

Leaman, K.D. and Molinari, R.L., 1987. Topographic modification of the Florida current by Little Bahama and Great Bahama Banks. J. Phys. Oceanogr., 17: 1724–1736.

Marchuk, G.I., Kordzadze, A.A. and Skiba, Y.N., 1975. Calculation of the basic hydrological fields in the Black Sea. Atmos. Ocean Phys., 11(4): 379–393.

Mee, L.D., 1992. The Black Sea in Crisis: the Need for Concerted International Action. Ambio.

Millot, C., 1991. Mesoscale and seasonal variabilities of the circulation in the Western Mediterranean. Dyn. Atmos. Oceans, 15: 179–214.

Moskalenko, L.V., 1976. Calculation of stationary wind driven currents in the Black Sea. Oceanology, 15: 168–171.

Murray, J.W., Codispoti, L.A. and Friederich, G.E., 1994. Redox Environments: The Suboxic Zone in the Black Sea. In: C.P. Huang, C.R. O'Melia and J.J. Morgan (Editors), Aquatic Chemistry, Advances in Chemistry Series, Am. Chem. Soc.

Musayeva, E.I., 1985. Mesoplankton near the Bulgarian coast. Oceanology, 25: 647–652.

Mysak, L.A. and Schott, F., 1977. Evidence for baroclinic instability of Norwegian current. J. Geophys. Res., 82: 2087–2095.

Neumann, G., 1942. Das Schwarze Meer. Z. Ges. Erdkunde, Berlin, 3: 92–114.

Niermann, U., Bingel, F., Gorban, A., Gordina, A.D., Gücü, A., Kideyş, A.E., Konsulov, A., Radu, G., Subbotin, A.A. and Zaika, V.E., 1993. Distribution of Anchovy Eggs and Larvae (*Engraulis encrasicolus* Cuv.) in the Black Sea in 1991 and 1992 in Comparison to Former Surveys, ICES, CM1993/H:48, 19 pp.

Okubo, A., 1980. Diffusion and Ecological Problems: Mathematical Models, Springer-Verlag, 254 pp.

Oğuz, T., La Violette, P.E. and Ünlüata, Ü., 1992. The upper layer circulation of the Black Sea: Its variability as inferred from hydrographic and satellite observations. J. Geophys. Res., 97: 12,569–12,584.

Oğuz, T., Latun, V.S., Latif, M.A., Vladimirov, V.V., Sur, H.İ., Markov, A.A., Özsoy, E., Kotovshchikov, B.B., Eremeev, V.V. and Ünlüata, Ü., 1993. Circulation in the surface and intermediate layers of the Black Sea. Deep-Sea Res., 40(8): 1597–1612.

Oğuz, T., Aubrey, D.G., Latun, V.S., Demirov, E., Koveshnikov, L., Sur, H.I., Diaconu, V., Besiktepe, S., Duman, M., Limeburner, R. and Eremeev, V., 1994. Mesoscale circulation and thermohaline structure of the Black Sea observed during HydroBlack 1991. Deep-Sea Res., 41(8): 603–628.

Oğuz, T., Aubrey, D.G., Besiktepe, S., Ivanov, L.I., Diacanu, V. and Ünlüata, Ü., 1995. On the ADCP observations of the western Black Sea Rim Current (submitted to Deep-Sea Res. II).

Özsoy, E., Latif, M.A., Tuğrul, S. and Ünlüata, Ü., 1992. Exchanges with the Mediterranean, Fluxes and Boundary mixing Processes in the Black Sea, presented at the Black Sea Symp. XXXIIIrd Cong. Plenary Assembly Int. Comm. Sci. Exploration of the Mediterranean Sea (CIESM), Trieste, 12–17 October 1992.

Özsoy, E., Ünlüata, Ü. and Top, Z., 1993. The mediterranean water evolution, material transport by double diffusive intrusions and interior mixing in the Black Sea. Prog. Oceanogr., 31: 279–320.

Qiu, B., Imasato, N. and Awaji, T., 1988. Baroclinic instability of buoyancy-driven coastal density currents. J. Geophys. Res., 93: 5037–5050.

Polat, S.G. and Tuğral, S., 1995. Nutrient and Organic Carbon Exchanges between the Black and Marmara Seas through the Bosphorus Strait. Continental Shelf Res., 15: 1115–1132.

Robinson, I.S., 1991. Satellite Oceanography. An Introduction for Oceanographers and Remote-Sensing Scientists. Ellis Horwood, Chichester, 455 pp.

Saydam, C., Tuğrul, S., Baştürk, Ö. and Oğuz, T., 1992. Identification of the oxic/anoxic interface by isopycnal surfaces in the Black Sea, Deep-Sea Res., 40: 1405–1412.

Sorokin, Yu.I., 1983. The Black Sea. In: B.H. Ketchum (Editor), Estuaries and Enclosed Seas. Ecosystems of the World. Elsevier, Amsterdam, pp. 253–292.

Spitz, Y.H. and Nof, D., 1991. Separation of boundary currents due to bottom topography. Deep-Sea Res., 38: 1–20.

Stanev, E.V., 1990. On the mechanisms of the Black Sea circulation. Earth-Sci. Rev., 28: 285–319.

Stern, M.E., 1980. Geostrophic fronts, bores breaking and blocking waves. J. Fluid Mech., 99: 687–703.

Sukhanova, I.N., Flint, M.V., Hibaum, G., Karamfilov, V., Kopylov, A.I., Matveeva, E., Rat'kova, T.N. and Sazhin, A.P., 1988. *Exuviaella cordata* red tide in Bulgarian coastal waters (May to June 1986). Mar. Biol., 99: 1–8.

Sur, H.I., Özsoy, E. and Ünlüata, U., 1994. Boundary current instabilities, upwelling, shelf mixing and euthrophication processes in the Black Sea. Prog. Oceanogr., 33: 249–302.

Tolmazin D., 1985. Changing coastal oceanography of the Black Sea. I: Northwestern Shelf. Prog. Oceanogr., 15: 217–276.

Tuğrul, S., Baştürk, Ö., Saydam, C. and Ylmaz, A., 1992. Changes in the hydrochemistry of the Black Sea inferred from water density profiles. Nature, 359: 137–139.

Tumantseva, N.I., 1985. Red tide in Black Sea. Oceanology, 25: 99–101.

Uysal, Z., 1993. A Preliminary Study on Some Plankters along the Turkish Black Sea Coast—Species Composition and Spatial Distribution. Ph.D. Thesis, Inst. Mar. Sci. Middle East Tech. Univ., Erdemli, İçel, Turkey, 138 pp.

Yentsch, C.S., 1984. Satellite representation of features of ocean circulation indicated by CZCS colorimetry. In: J.C.J. Nihoul (Editor), Remote Sensing of Shelf Sea Hydrodynamics. Elsevier, Amsterdam, pp. 336–354.